Multistatic Localization in the Absence of Transmitter Position

Yang Zhang, *Student Member, IEEE*, and K. C. Ho, *Fellow, IEEE*

***Abstract*—A multistatic system uses a transmitter to illuminate the object of interest and collects the reflected signal by a number of receivers to determine its location. In some scenarios such as passive coherent localization or for gaining flexibility, the position of the transmitter is not known. This paper investigates the use of the indirect path measurements reflected off the object alone, or together with the direct path measurements from the transmitter to receivers for locating the object in the absence of the transmitter position. We show that joint estimation of the object and transmitter positions from both the indirect and direct measurements can yield a better object location estimate than using the indirect measurements only by eliminating the dependency of the transmitter position. An algebraic closed-form solution is developed for the nonlinear problem of joint estimation and is shown analytically to achieve the Cramér–Rao lower bound performance under Gaussian noise over the small error region. To complete the study and gain insight, the optimal receiver placement in the absence of transmitter position is derived by minimizing the estimation confidence region or the mean-square estimation error for the object location. The performance lost due to unknown transmitter position under the optimal geometries is quantified. Simulations confirm well with the theoretical developments.**

***Index Terms*—Localization, multistatic, optimal geometry, time delay.**

I. Introduction

LOCALIZATION of an object, whether cooperative or non-cooperative, has been an interest area of research with numerous applications in wireless sensor network (WSN) [1]–[3], network localization and navigation (NLN) [4]–[6], communications [7], [8], radar and sonar [9]–[11], and many others. The goal of localization is to estimate the position of an object from a set of noisy measurements collected by a number of receivers (sensors), in an active or a passive manner. Localization can use time based measurements such as time-of-arrival (TOA) [12], [13] or time-difference-of-arrival (TDOA) [14], [15], or others including received signal strength (RSS) [16] or angle-of-arrival (AOA) [17], or a combination of them [18]–[20]. This work focuses on active localization for better control of the performance and on time based measurement as it often provides higher positioning accuracy.

Manuscript received January 1, 2019; revised May 20, 2019; accepted June 26, 2019. Date of publication July 22, 2019; date of current version August 10, 2019. The associate editor coordinating the review of this manuscript and approving it for publication was Prof. Stefano Tomasin. *(Corresponding author: K. C. Ho.)*

The authors are with the Department of Electrical Engineering and Computer Science, University of Missouri, Columbia, MO 65211 USA (e-mail: yzk48@mail.missouri.edu; hod@missouri.edu).

Digital Object Identifier 10.1109/TSP.2019.2929960

We shall consider the object to be localized is passive, meaning that it will not actively send out a signal to the sensors to locate itself. Rather, a transmitter capable of stamping the sent time emits a probing signal and a number of synchronous receivers collect the echo reflected off the object to identify the location. Such a multistatic [21] approach for localization offers more flexibility and better performance than the monostatic [10] counterpart. It has been widely used in sensor networks, radar, sonar, as well as MIMO radar [9], [22]–[26]. A multistatic system having multiple transmitters can yield excellent localization precision, superior observability and broad object range coverage [27].

A multistatic setting can produce two possible measurements between a transmit-receive pair [24], [28]. One is the indirect path time measurement resulted from signal propagation from the transmitter reflected by the object to the receiver. The other is the direct path time measurement from the line-of-sight propagation between the transmitter and receiver. Only the indirect measurement relates to the object location of interest. It defines an ellipsoidal curve (2-D) or surface (3-D) that the object lies with the transmitter and receiver positions as the foci [28]. The ellipsoids from a number of transmit-receive pairs intersect and yield an object location estimate. The multistatic approach for localization is sometimes termed as elliptic positioning [28].

Elliptic positioning has been an active research and many results are available from the literatures. Recently, [28] performed a thorough investigation of the achievable accuracy for elliptic localization. It also derived the optimal receiver placement when the number of receivers is even. [29] extended the optimal geometry analysis to a more general case for even or odd number of receivers, by minimizing the area of estimation confidence region. Regarding the estimation of the object location from elliptic measurements, [30] examined the spherical-intersection and spherical-interpolation methods and their positioning performance is only suboptimal. [31] proposed a BLUE estimator through linearizing the measurement equations by the Taylor series expansion and the estimator requires an accurate initial guess. [32] introduced a two-step estimator that is in closed-form when there is only one transmitter. [33] developed a similar closed-form solution under the in-door localization scenario. [34] and [35] extended the two-step estimator to multiple transmitters, where the former used the multidimensional scaling (MDS) framework and the latter applied the weighted least-squares (WLS) optimization from [14]. [36] derived an algebraic solution for sonar application where uncertainty appears in the signal propagation speed. The transmitter position is often

considered available in the elliptic localization literatures, although it may have some errors.

This paper addresses the scenario for elliptic positioning where the transmitter position is completely unavailable. Such a scenario appears when the transmitter is in some special inaccessible place. It also happens for the passive coherent location system in which the illumination signal is from some unknown radio source [37], [38]. Another situation is the position of the transmitter varies in time and its reported/estimated position is un-reliable. This is especially the case in sonar where the transmitter can be floating and drafting with the currents, making the previously estimated transmitter position not applicable. Indeed, the position of the transmitter can even be intentionally left unknown. Under such a setting, the transmitter operates as an illumination source only and its structure can be simplified, resulting in significantly lower hardware and implementation costs. For example, it allows an underwater WSN [39] to relieve a surface buoy of determining and sending its own position. An intuitive tactic of solving such a localization problem without the transmitter position is to perform the difference of two indirect measurements [40], [41], resulting in a time difference of arrival (TDOA) like measurement equation that is independent of the transmitter position, as the propagation time between the transmitter and the object is common among all the indirect path measurements. The resulting measurement value defines a hyperboloid instead of an ellipsoid for localization.

This paper takes a different approach for such a localization scenario by jointly estimating the object location and the transmitter position, although the transmitter position may not be of interest. Making use of both indirect and direct path measurements for joint estimation, we are able to demonstrate through the study via the Cramer-Rao Lower Bound (CRLB) the advantage of using joint estimation and the improvement in positioning accuracy compared to using the differencing approach. We next develop an algebraic closed-form solution to solve the highly nonlinear joint estimation problem, and show analytically in achieving the CRLB performance under Gaussian noise in the small error region. The solution is extended to the scenarios when sensor positions have random errors [25] and when multiple transmitters at unknown positions are present. Lastly, we derive the optimal receiver placement for elliptic localization when the transmitter position is not known. Both the optimization criteria of the estimation confidence region and the estimation mean square error (MSE) for the object location are considered. They yield slightly different configurations. The optimal placements enable us to characterize the lost in the best possible performance resulted from the transmitter position that is not known.

We illustrate the localization scenario in the next section. Section III evaluates the CRLB for the joint estimation, provides analysis and compares performance when using the differences of the indirect measurements or by introducing a new variable. Section IV proposes the new algebraic closed-form solution and analyzes the estimation accuracy. It also extends the solution to the situation when the receiver positions have errors and the use of multiple transmitters at unknown positions. Section V derives the optimal receiver placement for localization. Section VI presents the simulations and Section VII gives the conclusion.

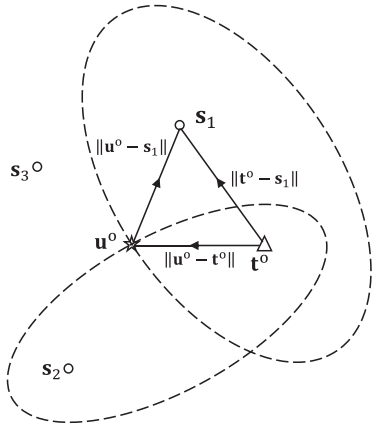

Fig. 1. Localization geometry.

Using common notations, bold uppercase letter and bold lowercase letter represent matrix and column vector. $\mathbf{a}(i:j)$ is a subvector containing the i-th to the j-th element of $\mathbf{a}$. $\mathrm{diag}(\mathbf{a})$ is a diagonal matrix formed by the elements of $\mathbf{a}$ and $\mathrm{diag}(\mathbf{A},\ldots,\mathbf{B})$ is a block diagonal matrix with diagonal blocks $\mathbf{A},\ldots,\mathbf{B}$. $\|\mathbf{a}\|$ is the Euclidean norm and $\boldsymbol{\rho}_{\mathbf{a}} = \mathbf{a}/\|\mathbf{a}\|$ is the unit length vector of $\mathbf{a}$. $\det(\mathbf{A})$ and $\mathrm{Tr}(\mathbf{A})$ are the determinant and the trace of $\mathbf{A}$. $\mathbf{I}$ and $\mathbf{O}$ are the identity and zero matrices with the size indicated by a subscript when needed. $\mathbf{1}_M$ and $\mathbf{0}_M$ are length M vectors of unity and zero, where the subscript maybe omitted if the size is clear from the context. The symbol $\otimes$ denotes the Kronecker product. $\mathbf{A} \succeq 0$ means $\mathbf{A}$ is positive semidefinite (PSD). $(*)^o$ is the true value of the variable or noisy quantity $(*)$.

II. Localization Scenario

Fig. 1 depicts a multistatic localization arrangement for locating an object using one transmitter and M receivers in a K dimensional space. The transmitter at unknown position $\mathbf{t}^o \in \mathbb{R}^K$ sends out a time stamped signal and it is reflected by the object at unknown position denoted by $\mathbf{u}^o \in \mathbb{R}^K$. Receiver i at known position $\mathbf{s}_i \in \mathbb{R}^K$ observes the indirect path signal through the object and the direct path signal from the transmitter, $i = 1, 2, \ldots, M$. We are interested in estimating the object position $\mathbf{u}^o$ using the indirect and direct path time delays where the transmitter position is not known.

The terms delay and range are used interchangeably as they are scaled version of each other by the known signal propagation speed. For the transmit-receive pair $(\mathbf{t}^o, \mathbf{s}_i)$, the true bistatic range (indirect path delay) is

$$r_i^o = \|\mathbf{u}^o - \mathbf{s}_i\| + \|\mathbf{u}^o - \mathbf{t}^o\| \tag{1}$$

and the true range between them (direct path delay) is

$$d_i^o = \|\mathbf{s}_i - \mathbf{t}^o\|. \tag{2}$$

The direct path delay is always smaller than the indirect path delay as illustrated in Fig. 1, which enables the distinction between them. The direct path delay does not depend on the object position and is usually ignored in the traditional multistatic localization, especially when the transmitter position is known.

The observations are corrupted by additive noise. The vector form of the indirect and direct path measurements are

$$\mathbf{r} = [r_1, r_2, \ldots, r_M]^T = \mathbf{r}^o + \boldsymbol{\varepsilon}_\mathbf{r}, \tag{3a}$$

$$\mathbf{d} = [d_1, d_2, \ldots, d_M]^T = \mathbf{d}^o + \boldsymbol{\varepsilon}_\mathbf{d}. \tag{3b}$$

$\boldsymbol{\varepsilon}_\mathbf{r} = [\varepsilon_{r1}, \varepsilon_{r2}, \ldots, \varepsilon_{rM}]^T$ and $\boldsymbol{\varepsilon}_\mathbf{d} = [\varepsilon_{d1}, \varepsilon_{d2}, \ldots, \varepsilon_{dM}]^T$ are uncorrelated zero-mean Gaussian noise vectors with known covariance matrices $\mathbf{Q}_\mathbf{r}$ and $\mathbf{Q}_\mathbf{d}$. The composite noise vector is $\boldsymbol{\varepsilon}_{\mathbf{r},\mathbf{d}} = [\boldsymbol{\varepsilon}_\mathbf{r}^T, \boldsymbol{\varepsilon}_\mathbf{d}^T]^T$ and it has the covariance matrix

$$\mathbf{Q} = \mathrm{diag}(\mathbf{Q}_\mathbf{r}, \mathbf{Q}_\mathbf{d}). \tag{4}$$

The developments mainly concentrate on the one transmitter case for ease of illustration. Extension of the study to the multiple transmitter scenario is elaborated in Section IV-D.

III. CRLB

The CRLB provides the performance limit of an unbiased estimator in terms of its covariance matrix. The localization problem we are addressing is nonlinear, leading to possibly a biased estimator. Nevertheless, when the noise level is not significant such that the bias is negligible compared to the estimation variance, the CRLB remains to be a good indicator for the maximum achievable accuracy [14], [28].

We shall consider three approaches to obtain the object location when the transmitter position $\mathbf{t}^o$ is not known. The first approach pre-processes the data measurement before estimation by forming the differences of multistatic ranges, thereby eliminating the transmitter position in the estimation process. The second approach introduces a nuisance variable that represents the distance between the object and the transmitter, and estimates the nuisance variable and the object location together. The third is more involved by joint estimation of the object and transmitter positions. Due to different parameterizations of the unknowns, the three approaches exploit the data measurements differently, resulting in separate estimation accuracy that can be revealed by the CRLB. We shall evaluate the CRLB for the source location of the three cases, and compare them through algebraic manipulation in the positive semidefinite viewpoint. The comparison provides insight about which of the three approaches yields the best localization accuracy of the object.

To proceed, let us define a few gradient matrices shown below:

$$\boldsymbol{\nabla}_\mathbf{u} = [\boldsymbol{\rho}_{\mathbf{u}^o-\mathbf{s}_1}, \boldsymbol{\rho}_{\mathbf{u}^o-\mathbf{s}_2}, \ldots, \boldsymbol{\rho}_{\mathbf{u}^o-\mathbf{s}_M}]^T, \tag{5a}$$

$$\boldsymbol{\nabla}_{\mathbf{rt}} = \frac{\partial \mathbf{r}^o}{\partial \mathbf{t}^{oT}} = [\boldsymbol{\rho}_{\mathbf{t}^o-\mathbf{u}^o}, \boldsymbol{\rho}_{\mathbf{t}^o-\mathbf{u}^o}, \ldots, \boldsymbol{\rho}_{\mathbf{t}^o-\mathbf{u}^o}]^T, \tag{5b}$$

$$\boldsymbol{\nabla}_{\mathbf{ru}} = \frac{\partial \mathbf{r}^o}{\partial \mathbf{u}^{oT}} = \boldsymbol{\nabla}_\mathbf{u} - \boldsymbol{\nabla}_{\mathbf{rt}}, \tag{5c}$$

$$\boldsymbol{\nabla}_{\mathbf{dt}} = \frac{\partial \mathbf{d}^o}{\partial \mathbf{t}^{oT}} = [\boldsymbol{\rho}_{\mathbf{t}^o-\mathbf{s}_1}, \boldsymbol{\rho}_{\mathbf{t}^o-\mathbf{s}_2}, \ldots, \boldsymbol{\rho}_{\mathbf{t}^o-\mathbf{s}_M}]^T. \tag{5d}$$

A. Multistatic Range Difference

Only the second term in (1) depends on the transmitter position $\mathbf{t}^o$ and it is common among all the indirect path range measurements. We can eliminate the unknown $\mathbf{t}^o$ by forming the difference $r_i - r_1$, $i = 2, 3, \ldots, M$, where r_1 (or any other one) acts as the reference for subtraction. $\mathbf{d}$ does not depend on $\mathbf{u}^o$ and has no use in this approach.

Let us denote the collection of the resulting differences by $\mathbf{q} \in \mathbb{R}^{M-1}$ and the differencing matrix by $\mathbf{H} \in \mathbb{R}^{M\times(M-1)}$

$$\mathbf{H} = [-\mathbf{1}_{M-1}, \mathbf{I}_{M-1}]^T. \tag{6}$$

$\mathbf{q}$ and its covariance matrix $\mathbf{Q}_\mathbf{q}$ are related to the indirect path measurement vector $\mathbf{r}$ and the original covariance matrix $\mathbf{Q}_\mathbf{r}$ by

$$\mathbf{q} = \mathbf{H}^T\mathbf{r}, \tag{7a}$$

$$\mathbf{Q}_\mathbf{q} = \mathbf{H}^T\mathbf{Q}_\mathbf{r}\mathbf{H}. \tag{7b}$$

Clearly $\mathbf{q}$ is Gaussian as premultiplying by $\mathbf{H}^T$ is a linear operation on the Gaussian vector $\mathbf{r}$. The logarithm of its probability density function parameterized by $\mathbf{u}^o$ is, after ignoring the constant term independent of the unknown,

$$\ln f_\mathbf{q}(\mathbf{q}\,;\,\mathbf{u}^o) = -\frac{1}{2}(\mathbf{q}-\mathbf{q}^o)^T\mathbf{Q}_\mathbf{q}^{-1}(\mathbf{q}-\mathbf{q}^o), \tag{8}$$

where $\mathbf{q}^o$ is the range difference vector as a function of $\mathbf{u}^o$ whose elements are $\|\mathbf{u}^o - \mathbf{s}_i\| - \|\mathbf{u}^o - \mathbf{s}_1\|$, $i = 2, 3, \ldots, M$. The CRLB of $\mathbf{u}^o$ is [42]

$$\mathrm{CRLB}_\mathbf{q}(\mathbf{u}^o) = -E\left[\frac{\partial^2 \ln f_\mathbf{q}}{\partial \mathbf{u}^o \partial \mathbf{u}^{oT}}\right]^{-1} = \left(\frac{\partial \mathbf{q}^{oT}}{\partial \mathbf{u}^o}\mathbf{Q}_\mathbf{q}^{-1}\frac{\partial \mathbf{q}^o}{\partial \mathbf{u}^{oT}}\right)^{-1}. \tag{9}$$

We have $\partial \mathbf{q}^o/\partial \mathbf{u}^{oT} = \mathbf{H}^T\boldsymbol{\nabla}_{\mathbf{ru}}$ from (7a) and (5c). Together with (7b), (9) becomes

$$\mathrm{CRLB}_\mathbf{q}(\mathbf{u}^o) = (\boldsymbol{\nabla}_{\mathbf{ru}}^T\mathbf{K}_\mathbf{q}\boldsymbol{\nabla}_{\mathbf{ru}})^{-1}, \tag{10}$$

where $\mathbf{K}_\mathbf{q}$ is

$$\mathbf{K}_\mathbf{q} = \mathbf{H}(\mathbf{H}^T\mathbf{Q}_\mathbf{r}\mathbf{H})^{-1}\mathbf{H}^T. \tag{11}$$

B. Using an Auxiliary Variable

Rather than using the differences, we keep the common scalar term in the indirect path range measurements and call it $\delta^o = \|\mathbf{u}^o - \mathbf{t}^o\|$ so that (1) becomes

$$r_i^o = \|\mathbf{u}^o - \mathbf{s}_i\| + \delta^o. \tag{12}$$

The unknown vector is considered as $[\mathbf{u}^{oT}, \delta^o]^T$. The direct path measurement vector $\mathbf{d}$ does not depend on the unknowns. From the Gaussian density of $\mathbf{r}$, the CRLB is

$$\mathrm{CRLB}_\mathbf{r}([\mathbf{u}^{oT}, \delta^o]^T) = \left(\left[\frac{\partial \mathbf{r}^o}{\partial \mathbf{u}^{oT}}, \frac{\partial \mathbf{r}^o}{\partial \delta^o}\right]^T\mathbf{Q}_\mathbf{r}^{-1}\left[\frac{\partial \mathbf{r}^o}{\partial \mathbf{u}^{oT}}, \frac{\partial \mathbf{r}^o}{\partial \delta^o}\right]\right)^{-1}. \tag{13}$$

From the model (12), we have $\partial \mathbf{r}^o/\partial \mathbf{u}^{oT} = \boldsymbol{\nabla}_\mathbf{u}$ in (5a) and $\partial \mathbf{r}^o/\partial \delta^o = \mathbf{1}_M$. Hence

$$\mathrm{CRLB}_\mathbf{r}([\mathbf{u}^{oT}, \delta^o]^T) = \begin{bmatrix}\mathbf{X}_\mathbf{r} & \mathbf{y}_\mathbf{r} \\ \mathbf{y}_\mathbf{r}^T & z_\mathbf{r}\end{bmatrix}^{-1} \tag{14}$$

where

$$\mathbf{X}_\mathbf{r} = \boldsymbol{\nabla}_\mathbf{u}^T\mathbf{Q}_\mathbf{r}^{-1}\boldsymbol{\nabla}_\mathbf{u}, \tag{15a}$$

$$\mathbf{y}_\mathbf{r} = \boldsymbol{\nabla}_\mathbf{u}^T\mathbf{Q}_\mathbf{r}^{-1}\mathbf{1}_M, \tag{15b}$$

$$z_\mathbf{r} = \mathbf{1}_M^T\mathbf{Q}_\mathbf{r}^{-1}\mathbf{1}_M. \tag{15c}$$

The CRLB for $\mathbf{u}^o$ is the upper left $K \times K$ block. Invoking the partitioned matrix inversion formula [42] yields

$$\mathrm{CRLB}_{\mathbf{r}}(\mathbf{u}^o) = \left(\mathbf{X}_{\mathbf{r}} - \mathbf{y}_{\mathbf{r}}\mathbf{y}_{\mathbf{r}}^T/z_{\mathbf{r}}\right)^{-1} . \tag{16}$$

Inserting $\mathbf{X}_{\mathbf{r}}$, $\mathbf{y}_{\mathbf{r}}$ and $z_{\mathbf{r}}$ defined by (15) results in

$$\mathrm{CRLB}_{\mathbf{r}}(\mathbf{u}^o) = \left(\boldsymbol{\nabla}_{\mathbf{u}}^T \mathbf{K}_{\mathbf{r}} \boldsymbol{\nabla}_{\mathbf{u}}\right)^{-1} , \tag{17}$$

where $\mathbf{K}_{\mathbf{r}}$ is

$$\mathbf{K}_{\mathbf{r}} = \mathbf{Q}_{\mathbf{r}}^{-1} - \mathbf{Q}_{\mathbf{r}}^{-1}\mathbf{1}_M(\mathbf{1}_M^T\mathbf{Q}_{\mathbf{r}}^{-1}\mathbf{1}_M)^{-1}\mathbf{1}_M^T\mathbf{Q}_{\mathbf{r}}^{-1} . \tag{18}$$

C. Joint Estimation

The unknown parameter vector is

$$\boldsymbol{\theta}^o = [\mathbf{u}^{oT}, \mathbf{t}^{oT}]^T. \tag{19}$$

The unknowns appear in both $\mathbf{r}$ and $\mathbf{d}$. Under Gaussian noise and uncorrelated $\mathbf{r}$ and $\mathbf{d}$,

$$\mathrm{CRLB}_{\mathbf{r},\mathbf{d}}(\boldsymbol{\theta}^o) = \left(\frac{\partial \mathbf{r}^{oT}}{\partial \boldsymbol{\theta}^o} \mathbf{Q}_{\mathbf{r}}^{-1} \frac{\partial \mathbf{r}^o}{\partial \boldsymbol{\theta}^{oT}} + \frac{\partial \mathbf{d}^{oT}}{\partial \boldsymbol{\theta}^o} \mathbf{Q}_{\mathbf{d}}^{-1} \frac{\partial \mathbf{d}^o}{\partial \boldsymbol{\theta}^{oT}} \right)^{-1} . \tag{20}$$

From (1) and (2) and with the notations in (5),

$$\frac{\partial \mathbf{r}^o}{\partial \boldsymbol{\theta}^{oT}} = [\, \boldsymbol{\nabla}_{\mathbf{ru}} \,,\, \boldsymbol{\nabla}_{\mathbf{rt}} \,] \quad , \quad \frac{\partial \mathbf{d}^o}{\partial \boldsymbol{\theta}^{oT}} = [\, \mathbf{O} \,,\, \boldsymbol{\nabla}_{\mathbf{dt}} \,] . \tag{21}$$

Thus,

$$\mathrm{CRLB}_{\mathbf{r},\mathbf{d}}(\boldsymbol{\theta}^o) = \begin{bmatrix} \mathbf{X} & \mathbf{Y} \\ \mathbf{Y}^T & \mathbf{Z} \end{bmatrix}^{-1} . \tag{22}$$

The submatrices are, using (5),

$$\mathbf{X} = \boldsymbol{\nabla}_{\mathbf{ru}}^T \mathbf{Q}_{\mathbf{r}}^{-1} \boldsymbol{\nabla}_{\mathbf{ru}} , \tag{23a}$$

$$\mathbf{Y} = \boldsymbol{\nabla}_{\mathbf{ru}}^T \mathbf{Q}_{\mathbf{r}}^{-1} \boldsymbol{\nabla}_{\mathbf{rt}} , \tag{23b}$$

$$\mathbf{Z} = \boldsymbol{\nabla}_{\mathbf{rt}}^T \mathbf{Q}_{\mathbf{r}}^{-1} \boldsymbol{\nabla}_{\mathbf{rt}} + \boldsymbol{\nabla}_{\mathbf{dt}}^T \mathbf{Q}_{\mathbf{d}}^{-1} \boldsymbol{\nabla}_{\mathbf{dt}} . \tag{23c}$$

Applying the block matrix inversion formula [42] gives

$$\mathrm{CRLB}_{\mathbf{r},\mathbf{d}}(\mathbf{u}^o) = \left(\boldsymbol{\nabla}_{\mathbf{ru}}^T [\, \mathbf{Q}_{\mathbf{r}}^{-1} - \mathbf{Q}_{\mathbf{r}}^{-1} \boldsymbol{\nabla}_{\mathbf{rt}} (\boldsymbol{\nabla}_{\mathbf{rt}}^T \mathbf{Q}_{\mathbf{r}}^{-1} \boldsymbol{\nabla}_{\mathbf{rt}} + \boldsymbol{\nabla}_{\mathbf{dt}}^T \mathbf{Q}_{\mathbf{d}}^{-1} \boldsymbol{\nabla}_{\mathbf{dt}})^{-1} \boldsymbol{\nabla}_{\mathbf{rt}}^T \mathbf{Q}_{\mathbf{r}}^{-1}] \boldsymbol{\nabla}_{\mathbf{ru}} \right)^{-1} .$$

If $(\boldsymbol{\nabla}_{\mathbf{dt}}^T \mathbf{Q}_{\mathbf{d}}^{-1} \boldsymbol{\nabla}_{\mathbf{dt}})$ is non-singular, invoking the Woodbury identity [42] to the matrix terms inside the square bracket gives the alternative form

$$\mathrm{CRLB}_{\mathbf{r},\mathbf{d}}(\mathbf{u}^o) = \left(\boldsymbol{\nabla}_{\mathbf{ru}}^T \mathbf{K}^{-1} \boldsymbol{\nabla}_{\mathbf{ru}} \right)^{-1} , \tag{24}$$

and

$$\mathbf{K} = \mathbf{Q}_{\mathbf{r}} + \boldsymbol{\nabla}_{\mathbf{rt}} (\boldsymbol{\nabla}_{\mathbf{dt}}^T \mathbf{Q}_{\mathbf{d}}^{-1} \boldsymbol{\nabla}_{\mathbf{dt}})^{-1} \boldsymbol{\nabla}_{\mathbf{rt}}^T . \tag{25}$$

The CRLB with known transmitter position is $(\boldsymbol{\nabla}_{\mathbf{ru}}^T \mathbf{Q}_{\mathbf{r}}^{-1} \boldsymbol{\nabla}_{\mathbf{ru}})^{-1}$. From (25), the absence of the transmitter location is equivalent to increasing the indirect path covariance matrix by an extra term that is dependent on the covariance matrix of the direct path and the relative positions among the object, transmitter and receivers.

D. Performance Comparison

The CRLB is a theoretical lower bound on the performance of an unbiased estimator and its trace gives the minimum possible estimation MSE. In general, localization approach $\mathcal{A}$ outperforms another approach $\mathcal{B}$ if $\mathrm{CRLB}_{\mathcal{B}} - \mathrm{CRLB}_{\mathcal{A}} \succeq 0$, meaning that the minimum uncertainty space of the estimate from $\mathcal{A}$ is inside that from $\mathcal{B}$. The positive semidefinite relation also implies $\mathrm{Tr}(\mathrm{CRLB}_{\mathcal{B}}) - \mathrm{Tr}(\mathrm{CRLB}_{\mathcal{A}}) \geq 0$.

1) $\mathrm{CRLB}_{\mathbf{q}}(\mathbf{u}^o)$ vs $\mathrm{CRLB}_{\mathbf{r}}(\mathbf{u}^o)$: The CRLB when using the range difference is given by (10)–(11), and that of using the indirect path range with the auxiliary variable δ^o is (17)–(18). We shall show that the two CRLBs are identical.

To begin, let us define $\widehat{\mathbf{H}} = \mathbf{Q}_{\mathbf{r}}^{\frac{1}{2}} \mathbf{H} \in \mathbb{R}^{M \times (M-1)}$ and $\widehat{\mathbf{1}} = \mathbf{Q}_{\mathbf{r}}^{-\frac{1}{2}} \mathbf{1} \in \mathbb{R}^{M \times 1}$, where $\mathbf{Q}_{\mathbf{r}}^{\frac{1}{2}}$ represents the square root of $\mathbf{Q}_{\mathbf{r}}$ such that $\mathbf{Q}_{\mathbf{r}}^{\frac{1}{2}} \mathbf{Q}_{\mathbf{r}}^{\frac{1}{2}} = \mathbf{Q}_{\mathbf{r}}$. The projection matrices onto their column spaces are

$$\mathbf{P}_{\widehat{\mathbf{H}}} = \widehat{\mathbf{H}} (\widehat{\mathbf{H}}^T \widehat{\mathbf{H}})^{-1} \widehat{\mathbf{H}}^T , \tag{26a}$$

$$\mathbf{P}_{\widehat{\mathbf{1}}} = \widehat{\mathbf{1}} (\widehat{\mathbf{1}}^T \widehat{\mathbf{1}})^{-1} \widehat{\mathbf{1}}^T . \tag{26b}$$

From (6) $\widehat{\mathbf{H}}^T \widehat{\mathbf{1}} = \mathbf{H}^T \mathbf{1} = \mathbf{0}_{M-1}$, meaning that $\widehat{\mathbf{1}}$ is orthogonal to the column space of $\widehat{\mathbf{H}}$. The two projection matrices span orthognal subspaces and they together compose the entire. Hence

$$\mathbf{P}_{\widehat{\mathbf{H}}} + \mathbf{P}_{\widehat{\mathbf{1}}} = \mathbf{I}_M . \tag{27}$$

Expressing $\widehat{\mathbf{H}}$ and $\widehat{\mathbf{1}}$ in terms of $\mathbf{H}$ and $\mathbf{1}$ from their definitions, pre- and post-multiplying by $\mathbf{Q}_{\mathbf{r}}^{-\frac{1}{2}}$ relates $\mathbf{K}_{\mathbf{q}}$ and $\mathbf{K}_{\mathbf{r}}$ defined in (11) and (18) by

$$\mathbf{K}_{\mathbf{q}} = \mathbf{K}_{\mathbf{r}} . \tag{28}$$

It is direct to validate from the definitions of $\mathbf{H}$ in (6) and $\boldsymbol{\nabla}_{\mathbf{rt}}$ in (5b) that

$$\mathbf{H}^T \boldsymbol{\nabla}_{\mathbf{rt}} = \mathbf{O}. \tag{29}$$

Hence using (5c)

$$\mathbf{H}^T \boldsymbol{\nabla}_{\mathbf{ru}} = \mathbf{H}^T \boldsymbol{\nabla}_{\mathbf{u}}. \tag{30}$$

Putting (11) into (10) and applying (28) and (30) yield immediately

$$\mathrm{CRLB}_{\mathbf{q}}(\mathbf{u}^o) = \mathrm{CRLB}_{\mathbf{r}}(\mathbf{u}^o) . \tag{31}$$

The localization performance of using the indirect path range differences turns out to be identical to that of introducing the auxiliary variable.

2) $\mathrm{CRLB}_{\mathbf{q}}(\mathbf{u}^o)$ vs $\mathrm{CRLB}_{\mathbf{r},\mathbf{d}}(\mathbf{u}^o)$: Let us begin with $\mathrm{CRLB}_{\mathbf{q}}(\mathbf{u}^o)$ for the comparison. Making use of (29), we can verify from (25)

$$\mathbf{H}^T \mathbf{K} \mathbf{H} = \mathbf{H}^T \mathbf{Q}_{\mathbf{r}} \mathbf{H}. \tag{32}$$

Putting it in (11), $\mathrm{CRLB}_{\mathbf{q}}(\mathbf{u}^o)$ in (10) can be expressed in terms of $\mathbf{K}$ by

$$\mathrm{CRLB}_{\mathbf{q}}(\mathbf{u}^o) = (\boldsymbol{\nabla}_{\mathbf{ru}}^T \mathbf{H} (\mathbf{H}^T \mathbf{K} \mathbf{H})^{-1} \mathbf{H}^T \boldsymbol{\nabla}_{\mathbf{ru}})^{-1} . \tag{33}$$

The matrix $\mathbf{K}$ in (25) is symmetric and positive definite, it has inverse and can be decomposed as $\mathbf{K} = \mathbf{K}^{\frac{1}{2}} \mathbf{K}^{\frac{1}{2}}$.

Let us define $\widetilde{\boldsymbol{\nabla}}_{\mathbf{ru}} = \mathbf{K}^{-\frac{1}{2}}\boldsymbol{\nabla}_{\mathbf{ru}} \in \mathbb{R}^{M\times K}$ and $\widetilde{\mathbf{H}} = \mathbf{K}^{\frac{1}{2}}\mathbf{H} \in \mathbb{R}^{M\times(M-1)}$. (33) and (24) can be rewritten as

$$\mathrm{CRLB}_{\mathbf{q}}(\mathbf{u}^o)^{-1} = \widetilde{\boldsymbol{\nabla}}_{\mathbf{ru}}^T\widetilde{\mathbf{H}}(\widetilde{\mathbf{H}}^T\widetilde{\mathbf{H}})^{-1}\widetilde{\mathbf{H}}^T\widetilde{\boldsymbol{\nabla}}_{\mathbf{ru}}\,, \tag{34}$$

$$\mathrm{CRLB}_{\mathbf{r},\mathbf{d}}(\mathbf{u}^o)^{-1} = \widetilde{\boldsymbol{\nabla}}_{\mathbf{ru}}^T\widetilde{\boldsymbol{\nabla}}_{\mathbf{ru}}\,, \tag{35}$$

where $\widetilde{\mathbf{H}}(\widetilde{\mathbf{H}}^T\widetilde{\mathbf{H}})^{-1}\widetilde{\mathbf{H}}^T$ is the projection matrix onto the column space of $\widetilde{\mathbf{H}}$. From the property of projection matrix [43],

$$\mathbf{I}_M - \widetilde{\mathbf{H}}(\widetilde{\mathbf{H}}^T\widetilde{\mathbf{H}})^{-1}\widetilde{\mathbf{H}}^T \succeq 0\,. \tag{36}$$

Pre- and post-multiplying it by $\widetilde{\boldsymbol{\nabla}}_{\mathbf{ru}}^T$ and $\widetilde{\boldsymbol{\nabla}}_{\mathbf{ru}}$ gives $\mathrm{CRLB}_{\mathbf{r},\mathbf{d}}(\mathbf{u}^o)^{-1} - \mathrm{CRLB}_{\mathbf{q}}(\mathbf{u}^o)^{-1} \succeq 0$, or equivalently,

$$\mathrm{CRLB}_{\mathbf{q}}(\mathbf{u}^o) \succeq \mathrm{CRLB}_{\mathbf{r},\mathbf{d}}(\mathbf{u}^o)\,. \tag{37}$$

In other words, joint localization using both the indirect and direct path measurements can often perform better than estimating the object location using the differences of the indirect path measurements. Identical performance only appears under some special geometries. Appendix A shows that such a configuration is that the transmitter and all receivers are collinear in 2-D positioning and coplanar in 3-D localization.

The following expression summarizes the relative performance of the three localization approaches:

$$\mathrm{CRLB}_{\mathbf{q}}(\mathbf{u}^o) = \mathrm{CRLB}_{\mathbf{r}}(\mathbf{u}^o) \succeq \mathrm{CRLB}_{\mathbf{r},\mathbf{d}}(\mathbf{u}^o)\,. \tag{38}$$

IV. Algebraic Closed-Form Solution

We would like to obtain a solution for the joint estimation of the object and transmitter positions. Both the indirect and direct measurements are nonlinearly related to the unknowns, making the estimation problem complicated to solve. While iterative solution is a possibility, it could be sensitive to the initial solution guesses and have divergence issue. We shall resort to an algebraic solution instead.

The proposed estimator follows the two-stage processing approach [14]. The first stage forms pseudolinear equation from the measurement model by introducing auxiliary variables as additional unknowns and solves it by the linear least-squares minimization. The second stage exploits the relationship between the auxiliary variables and the actual unknowns to refine the estimate.

The proposed solution essentially converts the nonlinear estimation problem to a linear form that enables the use of linear estimation technique for obtaining the solution. It inherently assumes the measurement noise is not significant. The approximations in the solution derivations come from ignoring the second and higher order noise terms, unless specified otherwise. As a result, the proposed solution is expected to achieve good performance only over the small error region.

We shall first derive the closed-form solution followed by an analysis to validate that the solution accuracy reaches the CRLB over the small error region. The solution is next extended to handle the presence of sensor position errors, and the use of multiple transmitters at unknown positions.

A. Algorithm

1) First Stage: Starting with the indirect path data model (1), moving $\|\mathbf{u}^o - \mathbf{t}^o\|$ from the right to the left and taking the square operation on both sides yield

$$r_i^{o2} - \|\mathbf{s}_i\|^2 + 2\mathbf{s}_i^T\mathbf{u}^o - 2\mathbf{u}^{oT}\mathbf{t}^o - 2r_i^o\|\mathbf{u}^o - \mathbf{t}^o\| + \|\mathbf{t}^o\|^2 = 0. \tag{39}$$

The true value r_i^o is not available. Substituting $r_i^o = r_i - \varepsilon_{ri}$ and realizing $r_i - \|\mathbf{u}^o - \mathbf{t}^o\| = \|\mathbf{u}^o - \mathbf{s}_i\| + \varepsilon_{ri}$, we obtain

$$\|\mathbf{u}^o - \mathbf{s}_i\|\,\varepsilon_{ri} \simeq \frac{1}{2}(r_i^2 - \|\mathbf{s}_i\|^2) + \mathbf{s}_i^T\mathbf{u}^o - \mathbf{u}^{oT}\mathbf{t}^o - r_i\|\mathbf{u}^o - \mathbf{t}^o\| + \frac{1}{2}\|\mathbf{t}^o\|^2\,, \tag{40}$$

where ε_{ri}^2 is neglected. For the direct path measurement, squaring both sides of (2) and using $d_i^o = d_i - \varepsilon_{di}$ give

$$\|\mathbf{s}_i - \mathbf{t}^o\|\,\varepsilon_{di} \simeq \frac{1}{2}(d_i^2 - \|\mathbf{s}_i\|^2) + \mathbf{s}_i^T\mathbf{t}^o - \frac{1}{2}\|\mathbf{t}^o\|^2\,, \tag{41}$$

in which $d^o = \|\mathbf{s}_i - \mathbf{t}^o\|$ is used and ε_{di}^2 ignored on the left side. We define the unknown vector as

$$\boldsymbol{\varphi}^o = \left[\,\mathbf{u}^{oT},\, \mathbf{t}^{oT},\, \mathbf{u}^{oT}\mathbf{t}^o,\, \|\mathbf{u}^o - \mathbf{t}^o\|,\, \|\mathbf{t}^o\|^2\,\right]^T. \tag{42}$$

Collecting the M equations from (40) and those from (41) produces the pseudolinear equations in matrix form

$$\mathbf{B}_{\mathbf{r}}\boldsymbol{\varepsilon}_{\mathbf{r}} = \mathbf{h}_{\mathbf{r}} - \mathbf{G}_{\mathbf{r}}\boldsymbol{\varphi}^o\,, \tag{43a}$$

$$\mathbf{B}_{\mathbf{d}}\boldsymbol{\varepsilon}_{\mathbf{d}} = \mathbf{h}_{\mathbf{d}} - \mathbf{G}_{\mathbf{d}}\boldsymbol{\varphi}^o\,. \tag{43b}$$

The matrices and vectors are defined as

$$\mathbf{B}_{\mathbf{r}} = \mathrm{diag}\left(\|\mathbf{u}^o - \mathbf{s}_1\|,\, \|\mathbf{u}^o - \mathbf{s}_2\|, \ldots, \|\mathbf{u}^o - \mathbf{s}_M\|\right), \tag{44a}$$

$$\mathbf{h}_{\mathbf{r}} = \frac{1}{2}\left[(r_1^2 - \|\mathbf{s}_1\|^2), \ldots, (r_M^2 - \|\mathbf{s}_M\|^2)\right]^T, \tag{44b}$$

$$\mathbf{G}_{\mathbf{r}} = [\mathbf{g}_{r_1},\, \mathbf{g}_{r_2}, \ldots, \mathbf{g}_{r_M}]^T, \tag{44c}$$

$$\mathbf{g}_{r_i} = \left[-\mathbf{s}_i^T,\, \mathbf{0}_K^T,\, 1,\, r_i,\, -\frac{1}{2}\right]^T, \tag{44d}$$

$$\mathbf{B}_{\mathbf{d}} = \mathrm{diag}\left(\|\mathbf{s}_1 - \mathbf{t}^o\|,\, \|\mathbf{s}_2 - \mathbf{t}^o\|, \ldots, \|\mathbf{s}_M - \mathbf{t}^o\|\right), \tag{44e}$$

$$\mathbf{h}_{\mathbf{d}} = \frac{1}{2}\left[(d_1^2 - \|\mathbf{s}_1\|^2), \ldots, (d_M^2 - \|\mathbf{s}_M\|^2)\right]^T, \tag{44f}$$

$$\mathbf{G}_{\mathbf{d}} = [\mathbf{g}_{d_1},\, \mathbf{g}_{d_2}, \ldots, \mathbf{g}_{d_M}]^T, \tag{44g}$$

$$\mathbf{g}_{d_i} = \left[\mathbf{0}_K^T,\, -\mathbf{s}_i^T,\, 0,\, 0,\, \frac{1}{2}\right]^T. \tag{44h}$$

Stacking (43a) and (43b) together gives

$$\mathbf{B}_1\boldsymbol{\varepsilon}_{\mathbf{r},\mathbf{d}} = \mathbf{h}_1 - \mathbf{G}_1\boldsymbol{\varphi}^o\,, \tag{45}$$

where

$$\mathbf{B}_1 = \mathrm{diag}(\mathbf{B}_{\mathbf{r}},\, \mathbf{B}_{\mathbf{d}})^T,\ \mathbf{h}_1 = [\mathbf{h}_{\mathbf{r}}^T,\, \mathbf{h}_{\mathbf{d}}^T]^T,\ \mathbf{G}_1 = [\mathbf{G}_{\mathbf{r}}^T,\, \mathbf{G}_{\mathbf{d}}^T]^T, \tag{46}$$

and $\boldsymbol{\varepsilon}_{\mathbf{r},\mathbf{d}}$ is defined below (3). Let us pretend the elements of $\boldsymbol{\varphi}^o$ are independent. Applying the WLS optimization to (45) gives

the estimate

$$\boldsymbol{\varphi} = (\mathbf{G}_1^T \mathbf{W}_1 \mathbf{G}_1)^{-1} \mathbf{G}_1^T \mathbf{W}_1 \mathbf{h}_1 \,. \tag{47}$$

$\mathbf{W}_1$ is the weighting matrix set according to the equation error and is equal to [42]

$$\mathbf{W}_1 = E[\mathbf{B}_1 \boldsymbol{\varepsilon}_{\mathbf{r},\mathbf{d}} \boldsymbol{\varepsilon}_{\mathbf{r},\mathbf{d}}^T \mathbf{B}_1^T]^{-1} = \left(\mathbf{B}_1 \mathbf{Q} \mathbf{B}_1^T\right)^{-1} \,. \tag{48}$$

Under the condition (C1) in (61), the noise in $\mathbf{G}_1$ is small enough to be neglected. Subtracting both sides of (47) by $\boldsymbol{\varphi}^o$, multiplying by the transpose and taking expectation give

$$\mathrm{cov}(\boldsymbol{\varphi}) \simeq (\mathbf{G}_1^T \mathbf{W}_1 \mathbf{G}_1)^{-1} \,. \tag{49}$$

2) Second Stage: The first stage supposes that the elements of $\boldsymbol{\varphi}^o$ defined in (42) are unrelated, but indeed only $\mathbf{u}^o$ and $\mathbf{t}^o$ are. The second stage improves the estimation accuracy by exploring their relations.

We shall express the elements of the first stage solution $\boldsymbol{\varphi}$ in terms of the two independent unknowns $\mathbf{u}^o$ and $\mathbf{t}^o$ in linear form. Rewriting it as $\boldsymbol{\varphi} = \boldsymbol{\varphi}^o + \boldsymbol{\varepsilon}_1$ where $\boldsymbol{\varepsilon}_1$ is the estimation error, from (42)

$$\boldsymbol{\varepsilon}_1(1:K) = \boldsymbol{\varphi}(1:K) - \mathbf{u}^o \,, \tag{50}$$

$$\boldsymbol{\varepsilon}_1(K+1:2K) = \boldsymbol{\varphi}(K+1:2K) - \mathbf{t}^o \,, \tag{51}$$

where K is the localization dimension. From (50) and (51), the true value of the element $2\boldsymbol{\varphi}(2K+1)$ can be expressed as $2\boldsymbol{\varphi}(2K+1) - 2\boldsymbol{\varepsilon}_1(2K+1) = 2\mathbf{u}^{oT}\mathbf{t}^o = (\boldsymbol{\varphi}(1:K) - \boldsymbol{\varepsilon}_1(1:K))^T \mathbf{t}^o + (\boldsymbol{\varphi}(K+1:2K) - \boldsymbol{\varepsilon}_1(K+1:2K))^T \mathbf{u}^o$ so that after rearranging the terms

$$\begin{aligned} &- \mathbf{t}^{oT}\boldsymbol{\varepsilon}_1(1:K) - \mathbf{u}^{oT}\boldsymbol{\varepsilon}_1(K+1:2K) + 2\boldsymbol{\varepsilon}_1(2K+1) \\ &\quad = 2\boldsymbol{\varphi}(2K+1) - \boldsymbol{\varphi}^T(K+1:2K)\mathbf{u}^o - \boldsymbol{\varphi}^T(1:K)\mathbf{t}^o \,. \end{aligned} \tag{52}$$

Expressing $\boldsymbol{\varphi}(2K+2) = \|\mathbf{u}^o - \mathbf{t}^o\| + \boldsymbol{\varepsilon}_1(2K+2)$, squaring both sides and ignoring the second order error term give

$$\begin{aligned} \boldsymbol{\varphi}^2(2K+2) \simeq \|\mathbf{u}^o\|^2 + \|\mathbf{t}^o\|^2 - 2\mathbf{u}^{oT}\mathbf{t}^o \\ + 2\|\mathbf{u}^o - \mathbf{t}^o\|\boldsymbol{\varepsilon}_1(2K+2). \end{aligned} \tag{53}$$

Using $\|\mathbf{u}^o\|^2 = (\boldsymbol{\varphi}(1:K) - \boldsymbol{\varepsilon}_1(1:K))^T \mathbf{u}^o$, $\|\mathbf{t}^o\|^2 = (\boldsymbol{\varphi}(K+1:2K) - \boldsymbol{\varepsilon}_1(K+1:2K))^T \mathbf{t}^o$ and $\mathbf{u}^{oT}\mathbf{t}^o = \boldsymbol{\varphi}(2K+1) - \boldsymbol{\varepsilon}_1(2K+1)$, we have

$$\begin{aligned} &- \mathbf{u}^{oT}\boldsymbol{\varepsilon}_1(1:K) - \mathbf{t}^{oT}\boldsymbol{\varepsilon}_1(K+1:2K) + 2\boldsymbol{\varepsilon}_1(2K+1) \\ &\quad + 2\|\mathbf{u}^o - \mathbf{t}^o\|\boldsymbol{\varepsilon}_1(2K+2) \simeq 2\boldsymbol{\varphi}(2K+1) + \boldsymbol{\varphi}^2(2K+2) \\ &\quad - \boldsymbol{\varphi}^T(1:K)\mathbf{u}^o - \boldsymbol{\varphi}^T(K+1:2K)\mathbf{t}^o. \end{aligned} \tag{54}$$

Pre-multiplying (51) by $-\mathbf{t}^{oT}$ and realizing that $\mathbf{t}^{oT}\mathbf{t}^o = \boldsymbol{\varphi}(2K+3) - \boldsymbol{\varepsilon}_1(2K+3)$, we obtain

$$\begin{aligned} &- \mathbf{t}^{oT}\boldsymbol{\varepsilon}_1(K+1:2K) + \boldsymbol{\varepsilon}_1(2K+3) \\ &\quad = \boldsymbol{\varphi}(2K+3) - \boldsymbol{\varphi}^T(K+1:2K)\mathbf{t}^o \,. \end{aligned} \tag{55}$$

Setting the unknown vector as $\boldsymbol{\theta}^o$ defined in (19), (50)–(55) form the linear matrix equation

$$\mathbf{B}_2 \boldsymbol{\varepsilon}_1 = \mathbf{h}_2 - \mathbf{G}_2 \boldsymbol{\theta}^o. \tag{56}$$

The matrices and vector for (56) are given by

$$\mathbf{B}_2 = \begin{bmatrix} \mathbf{I}_K & \mathbf{O}_{K\times K} & \mathbf{0}_K & \mathbf{0}_K & \mathbf{0}_K \\ \mathbf{O}_{K\times K} & \mathbf{I}_K & \mathbf{0}_K & \mathbf{0}_K & \mathbf{0}_K \\ -\mathbf{t}^{oT} & -\mathbf{u}^{oT} & 2 & 0 & 0 \\ -\mathbf{u}^{oT} & -\mathbf{t}^{oT} & 2 & 2\|\mathbf{u}^o - \mathbf{t}^o\| & 0 \\ \mathbf{0}_K^T & -\mathbf{t}^{oT} & 0 & 0 & 1 \end{bmatrix}, \tag{57a}$$

$$\begin{aligned} \mathbf{h}_2 = [&\boldsymbol{\varphi}^T(1:K), \boldsymbol{\varphi}^T(K+1:2K),\, 2\boldsymbol{\varphi}(2K+1), \\ &2\boldsymbol{\varphi}(2K+1) + \boldsymbol{\varphi}^2(2K+2),\, \boldsymbol{\varphi}(2K+3)]^T, \end{aligned} \tag{57b}$$

$$\mathbf{G}_2 = \begin{bmatrix} \mathbf{I}_K & \mathbf{O}_{K\times K} \\ \mathbf{O}_{K\times K} & \mathbf{I}_K \\ \boldsymbol{\varphi}^T(K+1:2K) & \boldsymbol{\varphi}^T(1:K) \\ \boldsymbol{\varphi}^T(1:K) & \boldsymbol{\varphi}^T(K+1:2K) \\ \mathbf{0}_K^T & \boldsymbol{\varphi}^T(K+1:2K) \end{bmatrix}. \tag{57c}$$

Applying the WLS optimization yields the final estimate

$$\boldsymbol{\theta} = (\mathbf{G}_2^T \mathbf{W}_2 \mathbf{G}_2)^{-1} \mathbf{G}_2^T \mathbf{W}_2 \mathbf{h}_2. \tag{58}$$

The ideal weighting matrix is $E[\mathbf{B}_2 \boldsymbol{\varepsilon}_1 \boldsymbol{\varepsilon}_1^T \mathbf{B}_2^T]^{-1}$. Using (49), we set it to the approximated version

$$\mathbf{W}_2 = \left(\mathbf{B}_2 (\mathbf{G}_1^T \mathbf{W}_1 \mathbf{G}_1)^{-1} \mathbf{B}_2^T\right)^{-1} \,. \tag{59}$$

The noise of $\mathbf{W}_2$ is negligible under (C1) in (61) and that of $\mathbf{G}_2$ can be ignored under (C2)–(C3). The covariance matrix of the estimate can be approximated by

$$\mathrm{cov}(\boldsymbol{\theta}) \simeq (\mathbf{G}_2^T \mathbf{W}_2 \mathbf{G}_2)^{-1} \,. \tag{60}$$

The weighting matrices $\mathbf{W}_1$ and $\mathbf{W}_2$ depend on the true object and transmitter positions. We shall first fix $\mathbf{B}_1$ to the identity matrix to generate $\mathbf{W}_1$ and obtain an initial estimate of $\boldsymbol{\varphi}$. Then a better $\mathbf{W}_1$ can be generated for a more accurate $\boldsymbol{\varphi}$ estimate. The true values $\mathbf{u}^o$ and $\mathbf{t}^o$ in $\mathbf{B}_2$ for $\mathbf{W}_2$ shall be approximated by using the solution $\boldsymbol{\varphi}$ from the first stage. Such approximations are reasonable as the WLS optimization is insensitive to the noise in the weighting matrix [44].

B. Analysis

We shall compare the theoretical covariance matrix of the proposed solution with the CRLB. The comparison is under the first order analysis where the second order noise term is negligible in the presence of the first order. Let us introduce the following small error conditions:

$$\begin{aligned} &\text{(C1) } \mathrm{diag}(\mathbf{r}^o)^{-1}\boldsymbol{\varepsilon}_{\mathbf{r}} \simeq \mathbf{0}, \\ &\text{(C2) } \mathrm{diag}(\mathbf{u}^o)^{-1}\boldsymbol{\varepsilon}_1(1:K) \simeq \mathbf{0} \text{ or } \boldsymbol{\varepsilon}_1(1:K) \simeq \mathbf{0}, \\ &\text{(C3) } \mathrm{diag}(\mathbf{t}^o)^{-1}\boldsymbol{\varepsilon}_1(K+1:2K) \simeq \mathbf{0} \text{ or } \boldsymbol{\varepsilon}_1(K+1:2K) \simeq \mathbf{0}. \end{aligned} \tag{61}$$

The first condition requires the indirect path range measurement noise be small relative to the true value. The second and third conditions demand the estimation errors for the object and transmitter locations from the first stage be small relative to the true values. All three conditions are satisfied over the small error region.

Under the small noise conditions, the approximation in (60) is valid. Substituting (59) and (48) into (60) yields

$$\text{cov}(\boldsymbol{\theta}) \simeq (\mathbf{G}_3^T \mathbf{Q}^{-1} \mathbf{G}_3)^{-1}, \tag{62}$$

where

$$\mathbf{G}_3 = \mathbf{B}_1^{-1} \mathbf{G}_1 \mathbf{B}_2^{-1} \mathbf{G}_2 . \tag{63}$$

Appendix B shows that under the three conditions (C1)–(C3),

$$\mathbf{G}_3 \simeq \left[\frac{\partial \mathbf{r}^{oT}}{\partial \boldsymbol{\theta}^o}, \frac{\partial \mathbf{d}^{oT}}{\partial \boldsymbol{\theta}^o} \right]^T . \tag{64}$$

Using it in (62) together with (4) yields

$$\text{cov}(\boldsymbol{\theta}) \simeq \left(\frac{\partial \mathbf{r}^{oT}}{\partial \boldsymbol{\theta}^o} \mathbf{Q}_{\mathbf{r}}^{-1} \frac{\partial \mathbf{r}^o}{\partial \boldsymbol{\theta}^{oT}} + \frac{\partial \mathbf{d}^{oT}}{\partial \boldsymbol{\theta}^o} \mathbf{Q}_{\mathbf{d}}^{-1} \frac{\partial \mathbf{d}^o}{\partial \boldsymbol{\theta}^{oT}} \right)^{-1} . \tag{65}$$

Comparing with (20) concludes

$$\text{cov}(\boldsymbol{\theta}) \simeq \text{CRLB}(\boldsymbol{\theta}^o). \tag{66}$$

Thus, under the conditions (C1)–(C3) and over the small error region, the proposed solution reaches the CRLB accuracy for Gaussian measurement noise.

C. Presence of Sensor Position Error

Often the receiving sensor positions cannot be known perfectly and the available values have random errors. Ignoring the sensor position errors can lead to significant performance degradation [45]. We shall extend the closed-form solution to account for receiver position errors.

Let us use $\widetilde{\mathbf{s}}_i$ to denote the available position of the i-th receiver. $\mathbf{s} = [\mathbf{s}_1^T, \mathbf{s}_2^T, \ldots, \mathbf{s}_M^T]^T$ and $\widetilde{\mathbf{s}} = [\widetilde{\mathbf{s}}_1^T, \widetilde{\mathbf{s}}_2^T, \ldots, \widetilde{\mathbf{s}}_M^T]^T$ represent the vector forms of the true receiver positions that are not known and the erroneous receiver positions that are available. The receiver position error vector is

$$\Delta\mathbf{s} = \widetilde{\mathbf{s}} - \mathbf{s}, \tag{67}$$

where $\Delta\mathbf{s} = [\Delta\mathbf{s}_1^T, \Delta\mathbf{s}_2^T, \ldots, \Delta\mathbf{s}_M^T]^T$ and $\Delta\mathbf{s}_i = \widetilde{\mathbf{s}}_i - \mathbf{s}_i$. We shall model $\Delta\mathbf{s}$ as zero-mean Gaussian distributed with known covariance matrix $\mathbf{Q}_{\mathbf{s}}$. Putting $\mathbf{s}_i = \widetilde{\mathbf{s}}_i - \Delta\mathbf{s}_i$ into (40) and (41), and with a high probability that the second-order position error terms are negligible compared to the linear error terms, the measurement equations can be approximated by

$$\begin{aligned} \|\mathbf{u}^o - \mathbf{s}_i\| \varepsilon_{ri} + (\mathbf{u}^o - \mathbf{s}_i)^T \Delta\mathbf{s}_i \simeq \frac{1}{2}(r_i^2 - \|\widetilde{\mathbf{s}}_i\|^2) \\ + \widetilde{\mathbf{s}}_i^T \mathbf{u}^o - \mathbf{u}^{oT}\mathbf{t}^o - r_i\|\mathbf{u}^o - \mathbf{t}^o\| + \frac{1}{2}\|\mathbf{t}^o\|^2, \end{aligned} \tag{68}$$

$$\begin{aligned} \|\mathbf{t}^o - \mathbf{s}_i\| \varepsilon_{di} + (\mathbf{t}^o - \mathbf{s}_i)^T \Delta\mathbf{s}_i \simeq \frac{1}{2}(d_i^2 - \|\widetilde{\mathbf{s}}_i\|^2) \\ + \widetilde{\mathbf{s}}_i^T \mathbf{t}^o - \frac{1}{2}\|\mathbf{t}^o\|^2. \end{aligned} \tag{69}$$

Collecting these measurement equations together yields

$$\mathbf{B}_{\mathbf{r}} \boldsymbol{\varepsilon}_{\mathbf{r}} + \mathbf{D}_{\mathbf{r}} \Delta\mathbf{s} = \widetilde{\mathbf{h}}_{\mathbf{r}} - \widetilde{\mathbf{G}}_{\mathbf{r}} \boldsymbol{\varphi}^o , \tag{70a}$$

$$\mathbf{B}_{\mathbf{d}} \boldsymbol{\varepsilon}_{\mathbf{d}} + \mathbf{D}_{\mathbf{d}} \Delta\mathbf{s} = \widetilde{\mathbf{h}}_{\mathbf{d}} - \widetilde{\mathbf{G}}_{\mathbf{d}} \boldsymbol{\varphi}^o , \tag{70b}$$

where $\boldsymbol{\varphi}^o$ is defined in (42) and $\mathbf{B}_{\mathbf{r}}$ and $\mathbf{B}_{\mathbf{d}}$ in (44a) and (44e). $\widetilde{\mathbf{h}}_{\mathbf{r}}, \widetilde{\mathbf{h}}_{\mathbf{d}}, \widetilde{\mathbf{G}}_{\mathbf{r}}$ and $\widetilde{\mathbf{G}}_{\mathbf{d}}$ are $\mathbf{h}_{\mathbf{r}}, \mathbf{h}_{\mathbf{d}}, \mathbf{G}_{\mathbf{r}}$ and $\mathbf{G}_{\mathbf{d}}$ given in (44) with $\mathbf{s}_i$ replaced by $\widetilde{\mathbf{s}}_i$. $\mathbf{D}_{\mathbf{r}} = \text{diag}((\mathbf{u}^o - \mathbf{s}_1)^T, (\mathbf{u}^o - \mathbf{s}_2)^T, \ldots, (\mathbf{u}^o - \mathbf{s}_M)^T)$ and $\mathbf{D}_{\mathbf{d}} = \text{diag}((\mathbf{s}_1 - \mathbf{t}^o)^T, (\mathbf{s}_2 - \mathbf{t}^o)^T, \ldots, (\mathbf{s}_M - \mathbf{t}^o)^T)$. Stacking (70a) and (70b) yields

$$\mathbf{B}_1 \boldsymbol{\varepsilon}_{\mathbf{r},\mathbf{d}} + \mathbf{D}_1 \Delta\mathbf{s} = \widetilde{\mathbf{h}}_1 - \widetilde{\mathbf{G}}_1 \boldsymbol{\varphi}^o , \tag{71}$$

where $\mathbf{B}_1$ and $\boldsymbol{\varepsilon}_{\mathbf{r},\mathbf{d}}$ are defined below (45), and $\mathbf{D}_1 = [\mathbf{D}_{\mathbf{r}}^T, \mathbf{D}_{\mathbf{d}}^T]^T$. $\widetilde{\mathbf{h}}_1$ and $\widetilde{\mathbf{G}}_1$ are $\mathbf{h}_1$ and $\mathbf{G}_1$ in (45) with $\mathbf{s}_i$ replaced by $\widetilde{\mathbf{s}}_i$. The WLS solution in the first-stage is

$$\boldsymbol{\varphi} = (\widetilde{\mathbf{G}}_1^T \widetilde{\mathbf{W}}_1 \widetilde{\mathbf{G}}_1)^{-1} \widetilde{\mathbf{G}}_1^T \widetilde{\mathbf{W}}_1 \widetilde{\mathbf{h}}_1 . \tag{72}$$

The weighting matrix $\widetilde{\mathbf{W}}_1$ is, from the equation error of (71),

$$\widetilde{\mathbf{W}}_1 = \left(\mathbf{B}_1 \mathbf{Q} \mathbf{B}_1^T + \mathbf{D}_1 \mathbf{Q}_{\mathbf{s}} \mathbf{D}_1^T\right)^{-1} . \tag{73}$$

The second-stage is not affected by the presence of receiver position errors. It is the same as in Section IV-A-2 and the final solution is (58).

The weighting matrix $\widetilde{\mathbf{W}}_1$ depends on the true object and transmitter positions. It is handled as for $\mathbf{W}_1$ by approximating $\mathbf{B}_{\mathbf{r}}$ and $\mathbf{B}_{\mathbf{d}}$ properly and setting $\mathbf{D}_1$ to zero to initialize $\widetilde{\mathbf{W}}_1$, and obtaining a better $\widetilde{\mathbf{W}}_1$ through an update.

D. Multiple Transmitters

It is common in multistatic system especially in sonar/radar to use multiple transmitters for increasing performance. We formulate the general case that all transmitter positions are not known. The situation that some transmitters are known can be easily accounted for in the proposed algorithm. We also consider the presence of receiver position errors. The accurate sensor position scenario is a special case by setting $\mathbf{Q}_{\mathbf{s}}$ to zero.

Let $\mathbf{t}_j^o$, $j = 1, 2, \ldots, N$ be the unknown position of the j-th transmitter. Each transmitter gives M indirect and M direct measurements. There are $2MN$ in total whose ideal values are

$$r_{i,j}^o = \|\mathbf{u}^o - \mathbf{s}_i\| + \|\mathbf{u}^o - \mathbf{t}_j^o\| , \tag{74a}$$

$$d_{i,j}^o = \|\mathbf{s}_i - \mathbf{t}_j^o\| , \tag{74b}$$

for $i = 1, 2, \ldots, M$ and $j = 1, 2, \ldots, N$. Each transmitter has the same set of pseudo linear matrix equations as in (70). Putting them together for all transmitters yields (71), where the matrices and vectors are defined in Appendix C, with $\mathbf{B}_{\mathbf{r}}$, $\mathbf{D}_{\mathbf{r}}$, $\mathbf{B}_{\mathbf{d}}$ and $\mathbf{D}_{\mathbf{d}}$ replaced by $\widetilde{\mathbf{B}}_{\mathbf{r}}$, $\widetilde{\mathbf{D}}_{\mathbf{r}}$, $\widetilde{\mathbf{B}}_{\mathbf{d}}$ and $\widetilde{\mathbf{D}}_{\mathbf{d}}$. The unknown vector in the first-stage now becomes

$$\begin{aligned} \widetilde{\boldsymbol{\varphi}}^o = [\, \mathbf{u}^{oT}, \mathbf{t}_1^{oT}, \mathbf{t}_2^{oT}, \ldots, \mathbf{t}_N^{oT}, \mathbf{u}^{oT}\mathbf{t}_1^o, \mathbf{u}^{oT}\mathbf{t}_2^o, \ldots, \\ \mathbf{u}^{oT}\mathbf{t}_N^o, \|\mathbf{u}^o - \mathbf{t}_1^o\|, \|\mathbf{u}^o - \mathbf{t}_2^o\|, \ldots, \|\mathbf{u}^o - \mathbf{t}_N^o\|, \\ \|\mathbf{t}_1^o\|^2, \|\mathbf{t}_2^o\|^2, \ldots, \|\mathbf{t}_N^o\|^2\,]^T \end{aligned} \tag{75}$$

and it has $K(N+1) + 3N$ variables. The solution is (72).

The unknown vector in the second-stage is

$$\widetilde{\boldsymbol{\theta}}^o = [\mathbf{u}^{oT}, \mathbf{t}_1^{oT}, \mathbf{t}_2^{oT}, \ldots, \mathbf{t}_N^{oT}]^T . \tag{76}$$

The solution is (58), where the relevant matrices and vector are now re-defined according to Appendix C.

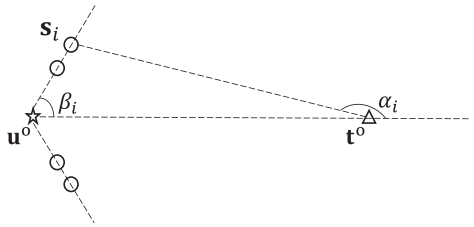

Fig. 2. Optimal geometry for 2-D joint localization.

V. Optimal Geometry

It is commonly known that the relative transmitter-object-sensor geometry is of great importance in network planning [4], [46], resource allocation [47]–[50], and target localization and tracking [51], [52], as it sets the limit on the achievable performance. This section derives the optimal receiver placement for the joint localization of the object and transmitter locations. To limit the scope, we shall consider the scenario of object localization with one transmitter and M receivers in the 2-D plane, where M is even. Following the previous studies [28] and [53], the measurement noise is IID such that

$$\mathbf{Q}_{\mathbf{r}} = \sigma_{\mathbf{r}}^2 \mathbf{I}_M, \mathbf{Q}_{\mathbf{d}} = \sigma_{\mathbf{d}}^2 \mathbf{I}_M. \tag{77}$$

Without loss of generality, we use $\mathbf{u}^o$ as the center point and set $\boldsymbol{\rho}_{\mathbf{t}^o-\mathbf{u}^o} = [1, 0]^T$ for coordinate reference. Let α_i and β_i be the bearing angles of the i-th receiver with respect to the transmitter and to the object as shown in Fig. 2 such that $\boldsymbol{\rho}_{\mathbf{s}_i-\mathbf{t}^o} = [\cos\alpha_i, \sin\alpha_i]^T$ and $\boldsymbol{\rho}_{\mathbf{s}_i-\mathbf{u}^o} = [\cos\beta_i, \sin\beta_i]^T$. The optimal geometry is defined by α_i and β_i, $i = 1, 2, \ldots, M$.

We shall use two criteria to derive the optimal receiver placement. One is the minimization of the localization confidence region which is equivalent to the maximization of the determinant of the FIM. The other is the minimization of the estimation MSE defined by the trace of the CRLB.

The FIM for the object location is given by (24), which is dependent on the matrix $\mathbf{K}$ in (25). Using (77) and substituting (5b) and (5d) give, in terms of α_i and β_i

$$\mathbf{K} = \sigma_{\mathbf{r}}^2 \mathbf{I}_M + \sigma_{\mathbf{d}}^2 \boldsymbol{\nabla}_{\mathbf{rt}} (\boldsymbol{\nabla}_{\mathbf{dt}}^T \boldsymbol{\nabla}_{\mathbf{dt}})^{-1} \boldsymbol{\nabla}_{\mathbf{rt}}^T = \sigma_{\mathbf{r}}^2 (\mathbf{I}_M + a \mathbf{1}_M \mathbf{1}_M^T). \tag{78}$$

The value a is caused by the transmitter position that is not known. It is dependent on the direct measurement noise power and the receiver-transmitter angle α_i and is always positive,

$$a = \frac{\sigma_{\mathbf{d}}^2}{\sigma_{\mathbf{r}}^2} \cdot \frac{\sum_{i=1}^M \sin^2 \alpha_i}{\sum_{i=1}^M \cos^2 \alpha_i \sum_{i=1}^M \sin^2 \alpha_i - (\sum_{i=1}^M \cos \alpha_i \sin \alpha_i)^2}. \tag{79}$$

The inverse of $\mathbf{K}$ is

$$\mathbf{K}^{-1} = \sigma_{\mathbf{r}}^{-2} (\mathbf{I}_M + b \mathbf{1}_M \mathbf{1}_M^T). \tag{80}$$

b relates to a through

$$b = -\frac{a}{1 + aM}, \tag{81}$$

and it is always negative. Applying (80) and using the angle representation for (5c), (24) becomes

$$\text{FIM}_{\mathbf{r},\mathbf{d}}(\mathbf{u}^o) = \sigma_{\mathbf{r}}^{-2} \begin{bmatrix} \upsilon_0 & \upsilon_1 \\ \upsilon_1 & \upsilon_2 \end{bmatrix}, \tag{82}$$

where

$$\upsilon_0 = b \left(\sum_{i=1}^M p_i \right)^2 + \sum_{i=1}^M p_i^2, \tag{83a}$$

$$\upsilon_1 = b \sum_{i=1}^M p_i \sum_{j=1}^M q_j + \sum_{i=1}^M p_i q_i, \tag{83b}$$

$$\upsilon_2 = b \left(\sum_{i=1}^M q_i \right)^2 + \sum_{i=1}^M q_i^2. \tag{83c}$$

In (83),

$$p_i = (1 + \cos\beta_i),\ q_i = \sin\beta_i, \tag{84}$$

and from trigonometry identity they are related by

$$q_i^2 = p_i(2 - p_i). \tag{85}$$

It is direct to validate

$$0 \le p_i \le 2. \tag{86}$$

Before proceeding further, let us first look at the worst case and the best case performance scenario caused by unknown transmitter position. The worst case appears when $\mathbf{K}$ is largest in the PSD sense, which is when a reaches the maximum value. It happens when the denominator of (79) becomes zero, resulted from $\cos\alpha_i = c \sin\alpha_i$ according to the Cauchy-Schwartz inequality [54], where c is a constant. Thus unknown transmitter position will degrade the localization accuracy most if the transmitter and all the receivers lie on a straight line. The corresponding smallest value of b from (81) is $-1/M$.

The best case happens when a is smallest, which is when

$$\sum_{i=1}^M \cos\alpha_i \sin\alpha_i = 0, \tag{87a}$$

$$|\cos\alpha_i| \to 1. \tag{87b}$$

The minimum possible value of a is

$$a_{min} = \frac{\sigma_{\mathbf{d}}^2}{\sigma_{\mathbf{r}}^2} \cdot \frac{1}{M}, \tag{88}$$

and the largest value of b is

$$b_{max} = -\frac{\sigma_{\mathbf{d}}^2}{\sigma_{\mathbf{r}}^2 + \sigma_{\mathbf{d}}^2} \cdot \frac{1}{M}. \tag{89}$$

A. Minimizing Estimation Confidence Region

The minimization is equivalent to the maximization of the determinant of $\text{FIM}_{\mathbf{r},\mathbf{d}}(\mathbf{u}^o)$ [29]. From (82), the determinant is

$$\zeta = \sigma_{\mathbf{r}}^{-4} (\upsilon_0 \upsilon_2 - \upsilon_1^2). \tag{90}$$

Let

$$\upsilon_2 = \upsilon_{2,1} + \upsilon_{2,2}\,,$$
$$\upsilon_{2,1} = b\left(\sum_{i=1}^{M} q_i\right)^2, \quad \upsilon_{2,2} = \sum_{i=1}^{M} q_i^2\,. \tag{91}$$

Then

$$\zeta = \sigma_{\mathbf{r}}^{-4}\left(\upsilon_0\upsilon_{2,1} + \upsilon_0\upsilon_{2,2} + (-\upsilon_1^2)\right)\,. \tag{92}$$

From (83a), υ_0 is a diagonal element of the FIM and cannot be negative. Recall that b given by (81) is negative. Hence the first term satisfies $\upsilon_0\upsilon_{2,1} \le 0$. Obviously the third term is $(-\upsilon_1^2) \le 0$. Let us consider maximizing the middle term which is always non-negative. Using (85) gives

$$(\upsilon_0\upsilon_{2,2}) = \left(b\left(\sum_{i=1}^{M} p_i\right)^2 + \sum_{i=1}^{M} p_i^2\right)\left(2\sum_{i=1}^{M} p_i - \sum_{i=1}^{M} p_i^2\right). \tag{93}$$

The derivatives of $(\upsilon_0\upsilon_{2,2})$ with respect to p_i, $i = 1, 2, \ldots, M$ yield the same expression, giving the relation

$$p_1 = p_2 = \cdots = p_M = p\,, \tag{94}$$

for reaching the maximum. Using (94) in (93), setting to zero the gradient with respect to p gives $p = 3/2$. Applying (84) then yields $\cos\beta_i = 1/2$ or $\beta_i = \pm 60$ deg. For even M, we can distribute the sensors evenly above and below the coordinate reference line $\mathbf{t}^o - \mathbf{u}^o$ so that

$$\beta_i = (-1)^i 60\,\text{deg}\,, \quad i = 1, 2, \ldots, M\,. \tag{95}$$

In such a case, from (84), we have $\sum_{i=1}^{M} q_i = 0$ and $\sum_{i=1}^{M} p_i q_i = 0$ such that from (83b) and (91) the negative terms $\upsilon_0\upsilon_{2,1}$ and $(-\upsilon_1^2)$ of (92) vanish. As a result, putting $p = 3/2$ back to (93) yields the maximum value

$$\zeta_{max} = \sigma_{\mathbf{r}}^{-4}\frac{27}{16}M^2(bM+1)\,. \tag{96}$$

It can be further optimized with respect to b. Clearly, it is increasing with b. The maximum value of b is given in (89), which is achieved when both conditions (87a) and (87b) are satisfied. To fulfill (87a), we require the receivers not only evenly but also symmetrically deployed on the two sides of the reference line and it will be satisfied under (95). The condition (87b) requires the receivers very close to or the transmitter far away from the object to maintain (95). The achievable maximum value of ζ is, when substituting (89),

$$\zeta_{max} = \sigma_{\mathbf{r}}^{-4}\frac{27}{16}M^2\left(\frac{\sigma_{\mathbf{r}}^2}{\sigma_{\mathbf{r}}^2 + \sigma_{\mathbf{d}}^2}\right)\,. \tag{97}$$

The corresponding optimal geometry is shown in Fig. 2, where β_i is given by (95) and α_i approaches ± 180 deg.

It should be noted that fulfilling the condition (87b) requires the indirect path and direct path delays have comparable values, implying the noise power $\sigma_{\mathbf{r}}^2 = \sigma_{\mathbf{d}}^2 = \sigma_{\boldsymbol{\varepsilon}}^2$ when the determinant of FIM is maximized. As a result ζ_{max} simplifies to

$$\zeta_{max} = \sigma_{\boldsymbol{\varepsilon}}^{-4}\frac{27}{32}M^2\,. \tag{98}$$

Comparing with the results from [29] where the transmitter position is known, the optimal receiver placement is the same. Nevertheless, ζ_{max} is reduced by a factor of two, which is equivalent to doubling the size of the confidence region.

B. Minimizing Estimation MSE

Tr(CRLB) is the minimum possible MSE of an unbiased estimator. Optimizing it will yield a configuration that has the best positioning accuracy in terms of MSE over the small error region where the bias is negligible compared to variance. $\text{CRLB}_{\mathbf{r},\mathbf{d}}(\mathbf{u}^o)$ is the inverse of $\text{FIM}_{\mathbf{r},\mathbf{d}}(\mathbf{u}^o)$. Minimizing Tr(CRLB) is equivalent to maximizing $1/\text{Tr(CRLB)}$. From (82)–(83), the objective for maximization is

$$\begin{aligned}\xi &= \frac{1}{\text{Tr}(\text{CRLB}_{\mathbf{r},\mathbf{d}}(\mathbf{u}^o))} = \frac{\det(\text{FIM}_{\mathbf{r},\mathbf{d}}(\mathbf{u}^o))}{\text{Tr}(\text{FIM}_{\mathbf{r},\mathbf{d}}(\mathbf{u}^o))} \\ &= \sigma_{\mathbf{r}}^{-2}\left(\frac{\upsilon_0\upsilon_2}{\upsilon_0+\upsilon_2} + \frac{-\upsilon_1^2}{\upsilon_0+\upsilon_2}\right)\,.\end{aligned} \tag{99}$$

The second term is negative. If we are able to maximize the first term while at the same time making the second term zero, ξ will reach the maximum value. Let us denote the first term inside the bracket of (99) by γ. After ignoring the constant $\sigma_{\mathbf{r}}^{-2}$ and using (91),

$$\gamma = \frac{\upsilon_0\upsilon_{2,1} + \upsilon_0\upsilon_{2,2}}{\upsilon_0 + \upsilon_{2,1} + \upsilon_{2,2}}\,. \tag{100}$$

It is monotonic increasing with $\upsilon_{2,1}$ since $\upsilon_0 + \upsilon_{2,1} + \upsilon_{2,2} = \text{Tr}(\text{FIM}_{\mathbf{r},\mathbf{d}}(\mathbf{u}^o)) \ge 0$. b is negative and $\upsilon_{2,1} \le 0$. γ is upper bounded by

$$\gamma \le \frac{\upsilon_0\upsilon_{2,2}}{\upsilon_0 + \upsilon_{2,2}}\,, \tag{101}$$

with the equality holds when $\upsilon_{2,1} = 0$. From (83) and using (85), in terms of the variables p_i,

$$\gamma \le \frac{\left(b\left(\sum_{i=1}^{M} p_i\right)^2 + \sum_{i=1}^{M} p_i^2\right)\left(2\sum_{i=1}^{M} p_i - \sum_{i=1}^{M} p_i^2\right)}{2\sum_{i=1}^{M} p_i + b\left(\sum_{i=1}^{M} p_i\right)^2}\,. \tag{102}$$

Due to the symmetric structure with respect to p_i, $i = 1, 2, \ldots, M$, we have (94) for attaining maximum on the right side. Keeping this requirement while at the same time distributing the receivers evenly above and below the reference line $\mathbf{u}^o - \mathbf{t}^o$, we have $\sum_{i=1}^{M} q_i = 0$ and $\sum_{i=1}^{M} p_i q_i = 0$ from (84) so that $\upsilon_1 = 0$ from (83b). Such an arrangement maintains (94) while at the same time making the second term $-\upsilon_1^2/(\upsilon_0+\upsilon_2)$ on the right side of (99) zero. Furthermore, equality holds for (101). As a result, the maximum value of ξ is the same as that of γ.

Using (94) in (102),

$$\gamma_{max} = M(bM+1)\frac{2p^2 - p^3}{bMp + 2}\,. \tag{103}$$

It can further be optimized. Taking the derivative with respect to p and setting it to zero result in

$$bMp^2 + (3 - bM)p - 4 = 0\,. \tag{104}$$

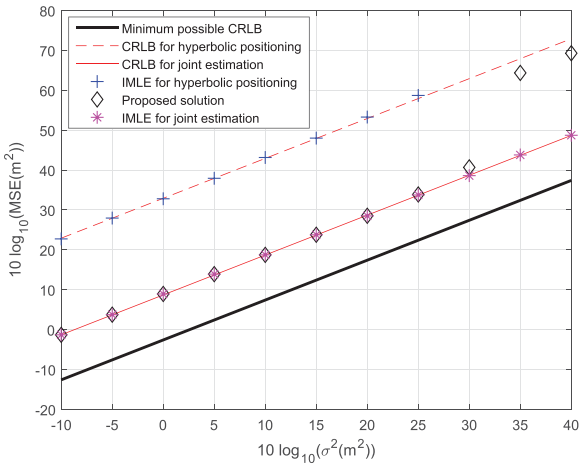

Fig. 3. Performance of the proposed solution with single transmitter and four receivers, compared with hyperbolic positioning.

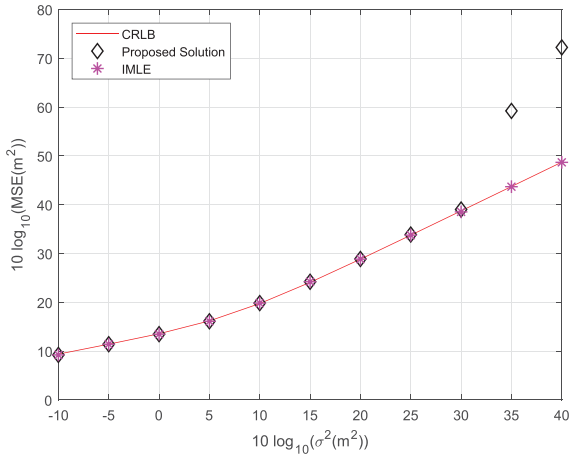

Fig. 4. Performance of the proposed solution in the presence of sensor position error at different measurement noise levels when $\sigma_{\mathbf{s}}^2 = 0.1\,\mathrm{m}^2$.

b is negative and the axis of symmetry of this quadratic equation is $(bM-3)/(2bM) \geq 2$ by considering the smallest value of b. Since $0 \leq p \leq 2$, the correct solution to (104) is given by

$$p = \frac{bM-3}{2bM} + \frac{\sqrt{(bM+1)(bM+9)}}{2bM}\,. \tag{105}$$

We next find the appropriate b to fix the solution (105).

It is direct to validate that γ_{max} is increasing with b, by taking the gradient of (103) with respect to b. Thus γ_{max} will reach the largest possible value by using b_{max} from (89), which requires (87a) and (87b) to be satisfied. (87a) is automatically fulfilled by the symmetric sensor arrangement. (87b) demands the transmitter far away from the sensors, which implies $\sigma_{\mathbf{r}}^2 = \sigma_{\mathbf{d}}^2 = \sigma_{\boldsymbol{\varepsilon}}^2$ and leads to $b_{max} = -1/(2M)$. Putting it back to (105) gives the solution of p as $p = (7-\sqrt{17})/2$. In other words, $\beta_i = \mathrm{acos}((5-\sqrt{17})/2) \simeq \pm 64\,\mathrm{deg}$, $i = 1, 2, \ldots, M$. Putting everything back to (99) gives the minimum value

$$\mathrm{Tr}(\mathrm{CRLB}_{\mathbf{r},\mathbf{d}}(\mathbf{u}^o)) \simeq \frac{2.2046}{M}\sigma_{\boldsymbol{\varepsilon}}^2\,. \tag{106}$$

The corresponding geometry is shown in Fig. 2, where β_i is

$$\beta_i = (-1)^i 64\,\mathrm{deg}\,, \quad i = 1, 2, \ldots, M\,, \tag{107}$$

and α_i approaches $\pm 180\,\mathrm{deg}$, $i = 1, 2, \ldots, M$.

If the transmitter position is known, [28] has determined the minimum achievable value for Tr(CRLB) is $(27/16)\sigma_{\boldsymbol{\varepsilon}}^2/M = 1.6875\,\sigma_{\boldsymbol{\varepsilon}}^2/M$, with the angle $\beta_i = 70.53\,\mathrm{deg}$. The performance lost resulted from unknown transmitter position is by the factor $2.2046/1.6875 = 1.3064 = 1.16\,\mathrm{dB}$.

Contrasting the results from the two optimization criteria, having an even number of receivers, both allocate them symmetrically on the two sides of the reference line $\mathbf{u}^o - \mathbf{t}^o$ and place them near the object. Half lie on a straight line passing through $\mathbf{u}^o$ and the other half another. The difference is that the first criterion requires the bearing angle of the receivers with respect to the object to be $|\beta_i| = 60\,\mathrm{deg}$ and the second criterion $|\beta_i| \simeq 64\,\mathrm{deg}$. The effect of unknown transmitter position results in a loss of 3 dB for the first criterion and 1.16 dB for the second.

VI. Simulation

In the simulation setting, the unit is meter for the position coordinates and the range measurements. It is square meter for the powers of the measurement noise and sensor position errors and for the MSE.

A. Joint Estimation

We evaluate localization performance through Monte-Carlo simulation with 2000 trials, in 2-D for ease of illustration. The results are shown in terms of the MSE between the object location estimate and the true position, in log-scale. The log-scale is used in order to cover a large dynamic range of estimation performance for better visualization.

We first consider locating an object at $\mathbf{u}^o = [2000,\ 5000]^T\,\mathrm{m}$ using one transmitter and four receivers whose positions are $\mathbf{t}^o = [0,\ 0]^T\,\mathrm{m}$, $\mathbf{s}_1 = [1000,\ 1000]^T\,\mathrm{m}$, $\mathbf{s}_2 = [1000,\ -1000]^T\,\mathrm{m}$, $\mathbf{s}_3 = [-1000,\ 1000]^T\,\mathrm{m}$ and $\mathbf{s}_4 = [-1000,\ -1000]^T\,\mathrm{m}$ [55]. The noise covariance matrix is given by (77) with $\sigma_{\mathbf{r}}^2 = \sigma_{\mathbf{d}}^2 = \sigma^2$. Fig. 3 illustrates the performance of the proposed estimator in terms of MSE as the measurement noise power σ^2 increases. Also shown is the performance of the Gauss-Newton iterative MLEs (IMLEs), initialized randomly from the area $[-10000,\ 10000]\,\mathrm{m} \times [-10000,\ 10000]\,\mathrm{m}$ for the joint estimation, and at the true object location for the hyperbolic approach described in Section III-A to ensure convergence before the thresholding effect happens. Both the proposed estimator and IMLE validate the significant performance advantage of joint estimation over the hyperbolic approach and reach the the CRLB performance from (24). The proposed estimator deviates from the CRLB earlier than IMLE. Nevertheless, it is about 2.5 times faster and does not have initialization issue. The minimum possible MSE when using 4 receivers from (106) is about 12 dB lower.

We next examine the performance of the proposed estimator in Section IV-C when sensor position errors are present having $\mathbf{Q}_{\mathbf{s}} = \sigma_{\mathbf{s}}^2\mathbf{J}$, where $\sigma_{\mathbf{s}}^2$ relates to the sensor position error power and $\mathbf{J} = \mathrm{diag}([5, 5, 40, 40, 20, 20, 10, 10]^T)$. Keeping $\sigma_{\mathbf{s}}^2$ at $0.1\,\mathrm{m}^2$, Fig. 4 confirms the proposed algorithm is able to reach the CRLB accuracy. Fig. 5 illustrates the results as the

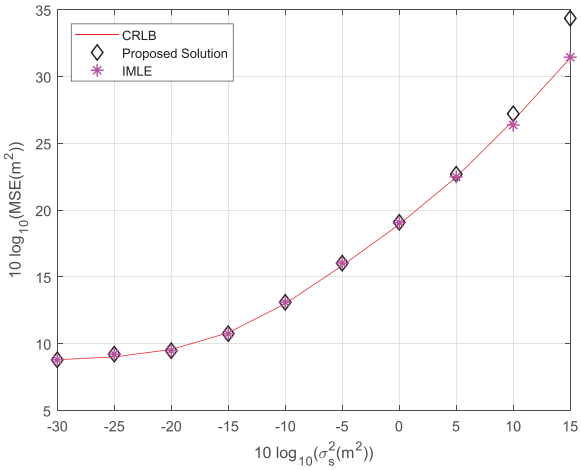

Fig. 5. Performance of the proposed solution in the presence of sensor position error at different levels of sensor position errors.

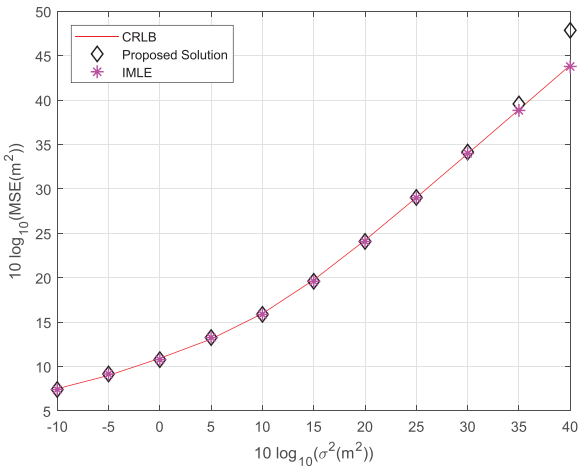

Fig. 6. Performance of the proposed solution in the presence of sensor position error using multiple transmitters.

sensor position error increases, at the measurement noise power $\sigma_{\mathbf{r}}^2 = \sigma_{\mathbf{d}}^2 = 1\,\mathrm{m}^2$. The proposed estimator attains the CRLB performance before the noise level becomes high and is 8 times faster than IMLE albeit deviating from the bound earlier.

Finally, we evaluate the estimation performance when using multiple transmitters at unknown positions. There are three transmitters whose true positions are $\mathbf{t}_1 = [-100,\ 0]^T$ m, $\mathbf{t}_2 = [100,\ 0]^T$ m and $\mathbf{t}_3 = [0,\ 100]^T$ m. The object and sensor locations are the same as before. The measurement noise and sensor position noise are independent with each other. The sensor position errors are having $\sigma_{\mathbf{s}}^2 = 0.1\,\mathrm{m}^2$. Fig. 6 shows that the proposed estimator in Section IV-D reaches the CRLB accuracy well, before the noise level becomes significant. It ran 13 times faster than IMLE in matlab implementation.

The proposed algorithm estimates the transmitter position in conjunction with the object position while the hyperbolic approach using the multistatic range differences does not. Table I compares the computation time of the proposed algorithm, the

TABLE I
COMPUTATIONAL COMPLEXITY COMPARISON FOR THE SIMULATION RESULTS IN FIG. 3

	Proposed Solution	IMLE/ Hyperbolic	IMLE/ Joint
Normalized Computation time	1	0.89	2.42

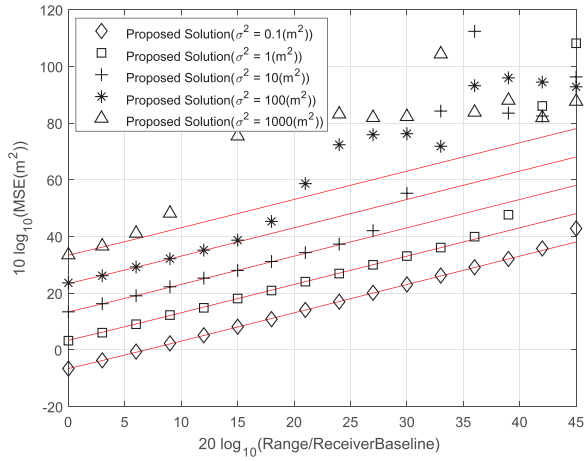

Fig. 7. Performance of the proposed solution as the object range relative to the receiver baseline increases under different noise levels.

IMLE for joint estimation and the IMLE for hyperbolic positioning. The algorithms were implemented using Matlab, running on an i7 processor with 8 GB memory. The computation times were recorded for the simulation in Fig. 3 with σ^2 varying from $0.1\,\mathrm{m}^2$ to $1000\,\mathrm{m}^2$, normalized by the processing time of the proposed algorithm. The proposed algorithm is more computationally efficient than IMLE for joint estimation. Experiments show that only when initialized at the true target position, the iterations for IMLE using the range differences for estimating the object location can be largely reduced, resulting in less computation time than the proposed algorithm. However, the running time will be substantially escalated if it is not initialized properly and the thresholding effect will appear early.

We have shown in Section IV-B that the proposed solution is able to achieve the CRLB performance over the small error region under Gaussian noise. Figs. 3–6 illustrate that the CRLB accuracy remains attainable by the proposed algorithm at high noise levels (low SNR in signal reception). Using the same receiver configuration in Fig. 3 while keeping the object angle at atan(2.5), Fig. 7 evaluates the performance of the proposed algorithm in a different perspective as the range of the object relative to the receiver baseline ($\sqrt{2} \times 2000\,\mathrm{m}$) increases, at range measurement noise power σ^2 equal to $[0.1,\ 1,\ 10,\ 100,\ 1000]\,\mathrm{m}^2$. As the noise power increases, the maximum object range that the proposed algorithm can yield the CRLB performance decreases. This is not unexpected as the noise tolerance reduces when the localization geometry becomes poor, i.e. the object is farther away from the receivers. The observations are similar in the presence of receiver position errors, as the proposed algorithm

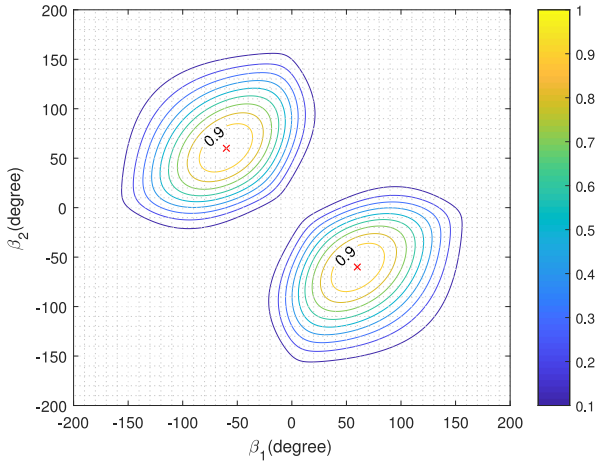

Fig. 8. Normalized $\det(\text{FIM}_{\mathbf{r},\mathbf{d}})$ as a function of β_1 and β_2.

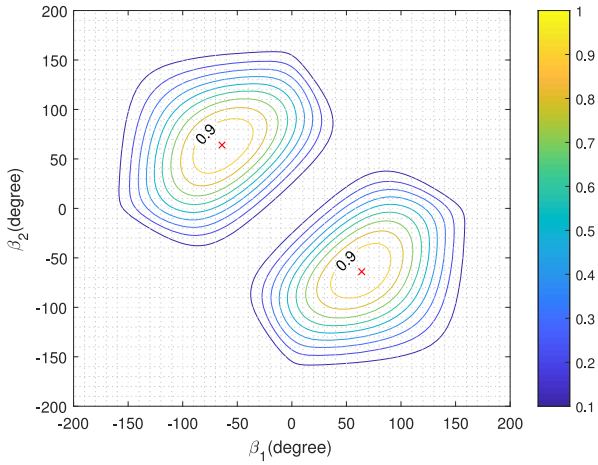

Fig. 9. Normalized $1/\text{Tr}(\text{CRLB}_{\mathbf{r},\mathbf{d}})$ as a function of β_1 and β_2.

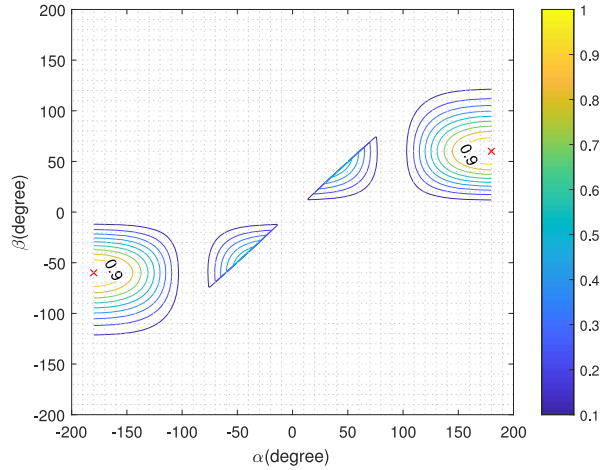

Fig. 10. Normalized $\det(\text{FIM}_{\mathbf{r},\mathbf{d}})$ as a function of α and β.

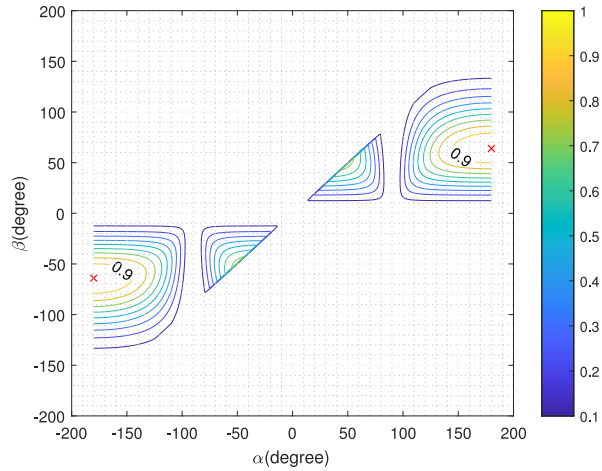

Fig. 11. Normalized $1/\text{Tr}(\text{CRLB}_{\mathbf{r},\mathbf{d}})$ as a function of α and β.

translates the receiver position errors to an increase in the range measurement noise.

B. Optimal Geometry

We shall validate the optimal geometries derived in Section V. The measurement noise is IID so that $\sigma_{\mathbf{r}}^2 = \sigma_{\mathbf{d}}^2$. The FIM determinant $\det(\text{FIM}_{\mathbf{r},\mathbf{d}}(\mathbf{u}^o))$ and the CRLB trace inverse $1/\text{Tr}(\text{CRLB}_{\mathbf{r},\mathbf{d}}(\mathbf{u}^o))$ are normalized by their maximum values for illustration.

First, we use two receivers to locate an object at $\mathbf{u}^o = [0,\, 0]^T$ m, with a transmitter at $\mathbf{t}^o = [100,\, 0]^T$ m. The receiver positions are $\mathbf{s}_i = [r\cos\beta_i,\, r\sin\beta_i]^T$ m, where β_i is the receiver-object bearing angle and $r = 10$ m for having the receivers near the object. The contour plots in Figs. 8 and 9 for $\det(\text{FIM}_{\mathbf{r},\mathbf{d}}(\mathbf{u}^o))$ and $1/\text{Tr}(\text{CRLB}_{\mathbf{r},\mathbf{d}}(\mathbf{u}^o))$ confirm the optimal angles (95) and (107) from the derivations.

Second, we use two receivers placed symmetrically with respect to the x-axis to locate an object at $\mathbf{u}^o = [0,\, 0]^T$ m with a transmitter at $\mathbf{t}^o = [1,\, 0]^T$ m. Figs. 10 and 11 give the contour plots of $\det(\text{FIM}_{\mathbf{r},\mathbf{d}}(\mathbf{u}^o))$ and $1/\text{Tr}(\text{CRLB}_{\mathbf{r},\mathbf{d}}(\mathbf{u}^o))$ as the receiver-transmitter angle α and receiver-object angle β vary. The former reaches the maximum value at $(\alpha = -180\,\text{deg},\, \beta = -60\,\text{deg})$ or $(\alpha = 180\,\text{deg},\, \beta = 60\,\text{deg})$, and the latter at $(\alpha = -180\,\text{deg},\, \beta = -64\,\text{deg})$ and $(\alpha = 180\,\text{deg},\, \beta = 64\,\text{deg})$. They validate the analysis that besides the conditions of (95) and (107), the optimal geometries also require the receiver-transmitter angle approaches ± 180 deg.

Next, we use two receivers to locate an object at $\mathbf{u}^o = [0,\, 0]^T$ m with a transmitter at $\mathbf{t}^o = [100,\, 0]^T$ m. The receiver positions are generated by $\mathbf{s}_1 = [r_1\cos\beta,\, r_1\sin\beta]^T$ m and $\mathbf{s}_2 = [r_2\cos\beta,\, -r_2\sin\beta]^T$ m, where $\beta = 60$ deg for $\det(\text{FIM}_{\mathbf{r},\mathbf{d}}(\mathbf{u}^o))$ and 64 deg for $1/\text{Tr}(\text{CRLB}_{\mathbf{r},\mathbf{d}}(\mathbf{u}^o))$. Figs. 12 and 13 illustrate their values as r_1 and r_2 vary. It confirms the receivers should be placed near the object. Even if the receivers are at 50 units away from the object, we still have around 90% of the maximum values of $\det(\text{FIM}_{\mathbf{r},\mathbf{d}}(\mathbf{u}^o))$ and $1/\text{Tr}(\text{CRLB}_{\mathbf{r},\mathbf{d}}(\mathbf{u}^o))$. From our study, it appears putting the receivers at half the distance away from the object as the transmitter would yield nearly the optimal results.

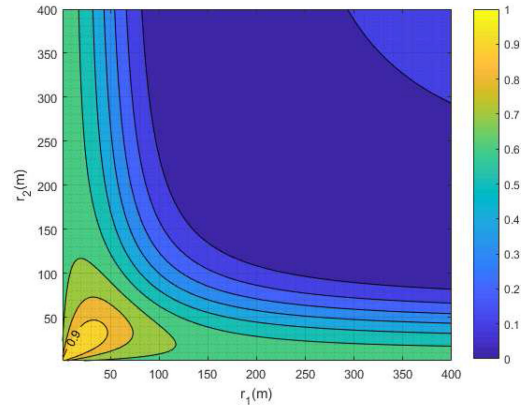

Fig. 12. Normalized $\det(\mathrm{FIM}_{\mathbf{r},\mathbf{d}})$ as a function of r_1 and r_2.

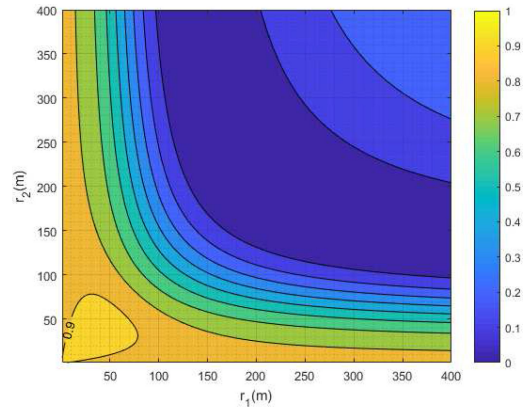

Fig. 13. Normalized $1/\mathrm{Tr}(\mathrm{CRLB}_{\mathbf{r},\mathbf{d}})$ as a function of r_1 and r_2.

TABLE II
GENETIC ALGORITHM SOLUTION FOR OPTIMAL GEOMETRY WITH FOUR RECEIVERS

criterion	r_1	r_2	r_3	r_4	β_1	β_2	β_3	β_4	d
$-\det(\mathrm{FIM}_{\mathbf{r},\mathbf{d}}(\mathbf{u}^o))$	2	2	2	2	$-60°$	$-60°$	$60°$	$60°$	100
$\mathrm{Tr}(\mathrm{CRLB}_{\mathbf{r},\mathbf{d}}(\mathbf{u}^o))$	2	2	2	2	$-64°$	$-64°$	$64°$	$64°$	100

At last, we use the genetic algorithm to find the minimum of $-\det(\mathrm{FIM}_{\mathbf{r},\mathbf{d}}(\mathbf{u}^o))$ and $\mathrm{Tr}(\mathrm{CRLB}_{\mathbf{r},\mathbf{d}}(\mathbf{u}^o))$ for further confirmation of the optimal geometries. There are four receivers at $\mathbf{s}_i = [r_i \cos\beta_i,\ r_i \sin\beta_i]^T$ m and a transmitter at $\mathbf{t}^o = [d,\ 0]^T$ m, and the object is at $\mathbf{u}^o = [0,\ 0]^T$ m. The optimization parameters are r_i, β_i for $i = 1, \ldots, 4$ and d, with their search ranges $2\,\mathrm{m} \le r_i \le 10\,\mathrm{m}$, $-\pi\,\mathrm{rad} \le \beta_i \le \pi\,\mathrm{rad}$ and $50\,\mathrm{m} \le d \le 100\,\mathrm{m}$. The maximum generation number of the genetic algorithm is 3000 and it stops if the average relative change of the best fitness function value over 50 generations is not larger than 10^{-15}. The numerical solutions for the two optimization criteria are shown in Table II. First, the results for receiver-object angles β_i validate (95) and (107). Second, $r_i = 2\,\mathrm{m}$ and $d = 100\,\mathrm{m}$ support the theoretical analysis that (i) the receivers should be deployed symmetrically on the two sides of the line joining $\mathbf{u}^o$ and $\mathbf{t}^o$, (ii) the receivers should be placed close to the object, and (iii) the transmitter should be far away from the object.

In practice, only some coarse estimate of the unknown location is available for design purpose, such as in resource allocation that exploits the uncertainty region of the object position formed by the coarse estimate [48]–[50]. For the problem of optimal receiver allocation, a coarse estimate of the object and transmitter locations may be sufficient if the objective measure is not sensitive to their exact optimal positions. The results in Fig. 10 and Fig. 11 show that the normalized $\det(\mathrm{FIM}_{\mathbf{r},\mathbf{d}})$ and $1/\mathrm{Tr}(\mathrm{CRLB}_{\mathbf{r},\mathbf{d}})$ remain large over a considerable region around the exact values of the optimal angles. In Fig. 10 for the $\det(\mathrm{FIM}_{\mathbf{r},\mathbf{d}})$ measure, the optimal angles are $(\alpha, \beta) = (180, 60)$ deg. The achievable $\det(\mathrm{FIM}_{\mathbf{r},\mathbf{d}})$ is within 90% of the best value for α within 145 to 180 deg and β within 47 to 73 deg. In Fig. 11 for the $1/\mathrm{Tr}(\mathrm{CRLB}_{\mathbf{r},\mathbf{d}})$ measure, the optimal angles are $(\alpha, \beta) = (180, 64)$ deg. The achievable $1/\mathrm{Tr}(\mathrm{CRLB}_{\mathbf{r},\mathbf{d}})$ is within 90% of the best value for α within 145 to 180 deg and β within 50 to 80 deg. We believe the optimal placement of the receiving sensors is not sensitive to the object and transmitter locations and their coarse estimates would be sufficient for achieving the (near) optimal receiver placement.

VII. CONCLUSION

This paper investigates a multistatic system to locate an object in which the transmitter position is not available. Starting from the fundamental study via the CRLB, we illustrate the performance improvement by using both the indirect and direct path measurements for joint estimation of the object and the transmitter position, in contrast to using the indirect measurement alone via the hyperbolic approach or by introducing a new variable for the transmitter-object distance. An algebraic closed-form solution is proposed to solve the nonlinear joint estimation problem, with the first order analysis in confirming the CRLB performance under Gaussian noise in the small error region. The algorithm is extended to account for receiver position errors as well as the use of multiple transmitters at unknown locations. We also derived the optimal receiver placement for such a localization system in the 2-D scenario when the number of receivers is even. The lost in the best achievable performance is 3dB when the optimal receiver placement criterion is the minimization of the estimation confidence region and is 1.16 dB when it is the minimization of the estimation MSE.

The proposed localization method assumes the transmitter is cooperative so that time stamp is available in the transmitted signal for the receivers to obtain the indirect and direct path range measurements. In the situation where the transmitter is not intentional such as for the passive coherent system, the signal sent time is often not known. If the transmitted signal has a well-defined pattern such as some standard synchronization or pilot sequence, it would still be able to estimate the indirect and direct path ranges but with an unknown constant offset added. The extension of such a situation is for our future research. The proposed method is not applicable for the non-cooperative transmitter scenario where the transmitted signal has no time stamp and does not have some known pattern.

APPENDIX A
GEOMETRY FOR IDENTICAL CRLBS WITH AND WITHOUT JOINT ESTIMATION

Without loss of generality, let

$$\boldsymbol{\rho}_{\mathbf{t}^o-\mathbf{u}^o} = [1,\, \mathbf{0}_{K-1}^T]^T, \tag{108}$$

and

$$\boldsymbol{\nabla}_{\mathbf{dt}}^T \mathbf{Q}_d^{-1} \boldsymbol{\nabla}_{\mathbf{dt}} = \begin{bmatrix} a & \mathbf{b}_{K-1}^T \\ \mathbf{b}_{K-1} & \mathbf{C}_{K-1\times K-1} \end{bmatrix}. \tag{109}$$

Then

$$\boldsymbol{\nabla}_{\mathbf{rt}} = \mathbf{1}_M \boldsymbol{\rho}_{\mathbf{t}^o-\mathbf{u}^o}^T = \mathbf{1}_M [1,\, \mathbf{0}_{K-1}^T]. \tag{110}$$

Putting $\boldsymbol{\nabla}_{\mathbf{rt}}$ and $\boldsymbol{\nabla}_{\mathbf{dt}}$ into $\mathbf{J} = \boldsymbol{\nabla}_{\mathbf{rt}} (\boldsymbol{\nabla}_{\mathbf{rt}}^T \mathbf{Q}_{\mathbf{r}}^{-1} \boldsymbol{\nabla}_{\mathbf{rt}} + \boldsymbol{\nabla}_{\mathbf{dt}}^T \mathbf{Q}_{\mathbf{d}}^{-1} \boldsymbol{\nabla}_{\mathbf{dt}})^{-1} \boldsymbol{\nabla}_{\mathbf{rt}}^T$ gives

$$\mathbf{J} = \mathbf{1}_M [1,\, \mathbf{0}_{K-1}^T] \begin{bmatrix} \mathbf{1}_M^T \mathbf{Q}_{\mathbf{r}}^{-1} \mathbf{1}_M + a & \mathbf{b}_{K-1}^T \\ \mathbf{b}_{K-1} & \mathbf{C}_{K-1\times K-1} \end{bmatrix}^{-1} \begin{bmatrix} 1 \\ \mathbf{0}_{K-1} \end{bmatrix} \mathbf{1}_M^T. \tag{111}$$

We shall show that under the following special geometries,

i) transmitter and receivers are colinear under the 2-D scenario,
ii) transmitter and receivers are coplanar under the 3-D scenario,

the CRLB for jointly estimating the transmitter and object locations is the same as that for estimating the object location only by forming the range differences.

Under the special geometry in (i) or (ii), the matrix in (109) is rank deficient, giving zero Schur complement of the block $\mathbf{C}$ in (109) such that

$$a = \mathbf{b}_{K-1}^T \mathbf{C}_{K-1\times K-1}^{-1} \mathbf{b}_{K-1}. \tag{112}$$

Here, we assume the transmitter, receivers and object in geometry (i) are not colinear, and they are not coplanar in geometry (ii). Besides, the transmitter and receivers in geometry (ii) are not colinear so that $\mathbf{C}$ is full rank and invertible. Should that be the case, we will not be able to locate a 2-D object with the configuration in (i) or a 3-D object with that in (ii).

Applying the block matrix inversion formula and using (112) yield immediately

$$\begin{aligned} \mathbf{J} &= \mathbf{1}_M (\mathbf{1}_M^T \mathbf{Q}_{\mathbf{r}}^{-1} \mathbf{1}_M + a - \mathbf{b}_{K-1}^T \mathbf{C}_{K-1\times K-1}^{-1} \mathbf{b}_{K-1})^{-1} \mathbf{1}_M^T \\ &= \mathbf{1}_M (\mathbf{1}_M^T \mathbf{Q}_r^{-1} \mathbf{1}_M)^{-1} \mathbf{1}_M^T. \end{aligned} \tag{113}$$

As a result, from the definition of $\mathbf{K}_{\mathbf{r}}$ in (18),

$$\mathbf{Q}_{\mathbf{r}}^{-1} - \mathbf{Q}_{\mathbf{r}}^{-1} \mathbf{J}^T \mathbf{Q}_{\mathbf{r}}^{-1} = \mathbf{K}_r. \tag{114}$$

Using (28) shows immediately that the CRLB of using range differences in (10) is identical to the CRLB (24) for joint estimation of the transmitter and object locations.

APPENDIX B
PROOF OF (64)

Substituting $\mathbf{B}_1 = \text{diag}(\mathbf{B}_{\mathbf{r}}, \mathbf{B}_{\mathbf{d}})^T$ and $\mathbf{G}_1 = [\mathbf{G}_{\mathbf{r}}^T, \mathbf{G}_{\mathbf{d}}^T]^T$ into (63) gives

$$\mathbf{G}_3 = \begin{bmatrix} \mathbf{B}_{\mathbf{r}}^{-1} \mathbf{G}_{\mathbf{r}} \\ \mathbf{B}_{\mathbf{d}}^{-1} \mathbf{G}_{\mathbf{d}} \end{bmatrix} \cdot \mathbf{B}_2^{-1} \mathbf{G}_2, \tag{115}$$

and $\mathbf{B}_{\mathbf{r}}$, $\mathbf{B}_{\mathbf{d}}$, $\mathbf{G}_{\mathbf{r}}$, $\mathbf{G}_{\mathbf{d}}$, $\mathbf{B}_2$ and $\mathbf{G}_2$ are given in (44) and (57).

Under (C1), the noise in $\mathbf{G}_1$ is negligible so that

$$\begin{aligned} &\mathbf{B}_{\mathbf{r}}^{-1} \mathbf{G}_{\mathbf{r}} = [\mathbf{b}_{r_1},\, \mathbf{b}_{r_2}, \ldots, \mathbf{b}_{r_M}]^T, \\ &\mathbf{b}_{r_i} \simeq \\ &\left[\frac{-\mathbf{s}_i^T}{\|\mathbf{u}^o - \mathbf{s}_i\|},\, \mathbf{0}_K^T,\, \frac{1}{\|\mathbf{u}^o - \mathbf{s}_i\|},\, \frac{r_i^o}{\|\mathbf{u}^o - \mathbf{s}_i\|},\, \frac{-1}{2\|\mathbf{u}^o - \mathbf{s}_i\|} \right]^T, \end{aligned} \tag{116}$$

$$\begin{aligned} &\mathbf{B}_{\mathbf{d}}^{-1} \mathbf{G}_{\mathbf{d}} = [\mathbf{b}_{d1},\, \mathbf{b}_{d2}, \ldots, \mathbf{b}_{dM}]^T, \\ &\mathbf{b}_{di} \simeq \left[\mathbf{0}_K^T,\, \frac{-\mathbf{s}_i^T}{\|\mathbf{t}^o - \mathbf{s}_i\|},\, 0,\, 0,\, \frac{1}{2\|\mathbf{t}^o - \mathbf{s}_i\|} \right]^T. \end{aligned} \tag{117}$$

Under (C2) and (C3), the noise in $\mathbf{G}_2$ is insignificant. As a result

$$\mathbf{B}_2^{-1} \mathbf{G}_2 \simeq \begin{bmatrix} \mathbf{I}_K & \mathbf{O}_{K\times K} \\ \mathbf{O}_{K\times K} & \mathbf{I}_K \\ \mathbf{t}^{oT} & \mathbf{u}^{oT} \\ \boldsymbol{\rho}_{\mathbf{u}^o-\mathbf{t}^o}^T & \boldsymbol{\rho}_{\mathbf{t}^o-\mathbf{u}^o}^T \\ \mathbf{0}_K^T & 2\mathbf{t}^{oT} \end{bmatrix}. \tag{118}$$

Direct multiplication gives

$$\mathbf{B}_{\mathbf{r}}^{-1} \mathbf{G}_{\mathbf{r}} \mathbf{B}_2^{-1} \mathbf{G}_2 = [\mathbf{p}_{r1},\, \mathbf{p}_{r2}, \ldots, \mathbf{p}_{rM}]^T, \tag{119a}$$

$$\mathbf{p}_{ri} \simeq [\boldsymbol{\rho}_{\mathbf{u}^o-\mathbf{s}_i}^T + \boldsymbol{\rho}_{\mathbf{u}^o-\mathbf{t}^o}^T,\, -\boldsymbol{\rho}_{\mathbf{u}^o-\mathbf{t}^o}^T]^T = \frac{\partial r_i^o}{\partial \boldsymbol{\theta}^{oT}},$$

$$\mathbf{B}_{\mathbf{d}}^{-1} \mathbf{G}_{\mathbf{d}} \mathbf{B}_2^{-1} \mathbf{G}_2 = [\mathbf{p}_{d1},\, \mathbf{p}_{d2}, \ldots, \mathbf{p}_{dM}]^T, \tag{119b}$$

$$\mathbf{p}_{di} \simeq [\mathbf{0}_K^T,\, \boldsymbol{\rho}_{\mathbf{t}^o-\mathbf{s}_i}^T]^T = \frac{\partial d_i^o}{\partial \boldsymbol{\theta}^{oT}}.$$

We have $\mathbf{B}_{\mathbf{r}}^{-1} \mathbf{G}_{\mathbf{r}} \mathbf{B}_2^{-1} \mathbf{G}_2 \simeq \partial \mathbf{r}^o / \partial \boldsymbol{\theta}^T$ and $\mathbf{B}_{\mathbf{d}}^{-1} \mathbf{G}_{\mathbf{d}} \mathbf{B}_2^{-1} \mathbf{G}_2 \simeq \partial \mathbf{d}^o / \partial \boldsymbol{\theta}^T$, putting them in (115) yields (64).

APPENDIX C
DETAILS FOR THE CLOSED-FORM ESTIMATOR WITH MULTIPLE TRANSMITTERS

A. Matrices for the First Stage

They are defined as follows:

$$\widetilde{\mathbf{B}}_{\mathbf{r}} = \mathbf{I}_N \otimes \mathbf{B}_{\mathbf{r}}, \tag{120a}$$

$$\widetilde{\mathbf{B}}_{\mathbf{d}} = \text{diag}(\mathbf{B}_{\mathbf{d},1},\, \mathbf{B}_{\mathbf{d},2}, \ldots, \mathbf{B}_{\mathbf{d},N}), \tag{120b}$$

$$\mathbf{B}_{\mathbf{d},j} = \text{diag}\left([\, \|\mathbf{s}_1 - \mathbf{t}_j^o\|,\, \|\mathbf{s}_2 - \mathbf{t}_j^o\|, \ldots, \|\mathbf{s}_M - \mathbf{t}_j^o\| \,] \right), \tag{120c}$$

$$\widetilde{\mathbf{D}}_{\mathbf{r}} = \mathbf{1}_N \otimes \mathbf{D}_{\mathbf{r}},$$

$$\mathbf{D}_{\mathbf{r}} = \text{diag}\left((\mathbf{u}^o - \mathbf{s}_1)^T, (\mathbf{u}^o - \mathbf{s}_2)^T, \ldots, (\mathbf{u}^o - \mathbf{s}_M)^T\right),$$

$$\widetilde{\mathbf{D}}_{\mathbf{d}} = \left[\mathbf{D}_{\mathbf{d},1}^T, \mathbf{D}_{\mathbf{d},2}^T, \ldots, \mathbf{D}_{\mathbf{d},N}^T\right]^T, \tag{120d}$$

$$\mathbf{D}_{\mathbf{d},j} = \text{diag}\left((\mathbf{s}_1 - \mathbf{t}_j^o)^T, (\mathbf{s}_2 - \mathbf{t}_j^o)^T, \ldots, (\mathbf{s}_M - \mathbf{t}_j^o)^T\right),$$

$$\widetilde{\mathbf{h}}_{\mathbf{r}} = [\mathbf{h}_{\mathbf{r},1}^T, \mathbf{h}_{\mathbf{r},2}^T, \ldots, \mathbf{h}_{\mathbf{r},N}^T]^T, \tag{120e}$$

$$\mathbf{h}_{\mathbf{r},j} = \frac{1}{2}\left[(r_{1,j}^2 - \|\widetilde{\mathbf{s}}_1\|^2), \ldots, (r_{M,j}^2 - \|\widetilde{\mathbf{s}}_M\|^2)\right]^T,$$

$$\widetilde{\mathbf{h}}_{\mathbf{d}} = [\mathbf{h}_{\mathbf{d},1}^T, \mathbf{h}_{\mathbf{d},2}^T, \ldots, \mathbf{h}_{\mathbf{d},N}^T]^T, \tag{120f}$$

$$\mathbf{h}_{\mathbf{d},j} = \frac{1}{2}\left[(d_{1,j}^2 - \|\widetilde{\mathbf{s}}_1\|^2), \ldots, (d_{M,j}^2 - \|\widetilde{\mathbf{s}}_M\|^2)\right]^T,$$

$$\widetilde{\mathbf{G}}_{\mathbf{r}} = [-\mathbf{1}_N \otimes \widetilde{\mathbf{S}}, \mathbf{O}_{MN\times NK}, \mathbf{I}_N \otimes \mathbf{1}_M, \text{diag}(\widetilde{\mathbf{r}}_1, \widetilde{\mathbf{r}}_2, \ldots, \widetilde{\mathbf{r}}_N), -\frac{1}{2}\mathbf{I}_N \otimes \mathbf{1}_M]^T, \tag{120g}$$

$$\widetilde{\mathbf{r}}_j = [r_{1,j}, r_{2,j}, \ldots, r_{M,j}]^T,$$

$$\widetilde{\mathbf{G}}_{\mathbf{d}} = \left[\mathbf{O}_{MN\times K}, -\mathbf{I}_N \otimes \widetilde{\mathbf{S}}, \mathbf{O}_{MN\times 2N}, \frac{1}{2}\mathbf{I}_N \otimes \mathbf{1}_M\right]^T, \tag{120h}$$

$$\widetilde{\mathbf{S}} = [\widetilde{\mathbf{s}}_1, \widetilde{\mathbf{s}}_2, \ldots, \widetilde{\mathbf{s}}_M]^T.$$

B. Matrices for the Second Stage

They are given by

$$\mathbf{B}_2 = \begin{bmatrix} \mathbf{I}_K & \mathbf{O}_{K\times KN} & \mathbf{O}_{K\times N} & \mathbf{O}_{K\times N} & \mathbf{O}_{K\times N} \\ \mathbf{O}_{KN\times K} & \mathbf{I}_{KN} & \mathbf{O}_{KN\times N} & \mathbf{O}_{KN\times N} & \mathbf{O}_{KN\times N} \\ -\mathbf{T}(\mathbf{1}_N \otimes \mathbf{I}_K) & -\mathbf{I}_N \otimes \mathbf{u}^{oT} & 2\mathbf{I}_N & \mathbf{O}_{N\times N} & \mathbf{O}_{N\times N} \\ -\mathbf{1}_N\mathbf{u}^{oT} & -\mathbf{T} & 2\mathbf{I}_N & 2\boldsymbol{\Delta} & \mathbf{O}_{N\times N} \\ \mathbf{O}_{N\times K} & -\mathbf{T} & \mathbf{O}_{N\times N} & \mathbf{O}_{N\times N} & \mathbf{I}_N \end{bmatrix}, \tag{121a}$$

$$\boldsymbol{\Delta} = \text{diag}\left(\left[\|\mathbf{u}^o - \mathbf{t}_1^o\|, \|\mathbf{u}^o - \mathbf{t}_2^o\|, \ldots, \|\mathbf{u}^o - \mathbf{t}_N^o\|\right]\right),$$

$$\mathbf{T} = \text{diag}\left(\mathbf{t}_1^{oT}, \mathbf{t}_2^{oT}, \ldots, \mathbf{t}_N^{oT}\right),$$

$$\mathbf{h}_2 = [\widetilde{\boldsymbol{\varphi}}(1:K)^T, \widetilde{\boldsymbol{\varphi}}(K+1:K(N+1))^T, 2\widetilde{\boldsymbol{\varphi}}(K(N+1)+1:K(N+1)+N)^T, \widetilde{\boldsymbol{\varphi}}^2((K+1)(N+1):K(N+1)+2N)^T + 2\widetilde{\boldsymbol{\varphi}}(K(N+1)+1:K(N+1)+N)^T, \widetilde{\boldsymbol{\varphi}}(K(N+1)+2N+1:K(N+1)+3N)^T]^T, \tag{121b}$$

$$\mathbf{G}_2 = \begin{bmatrix} \mathbf{I}_K & \mathbf{O}_{K\times KN} \\ \mathbf{O}_{KN\times K} & \mathbf{I}_{KN} \\ \widehat{\mathbf{T}}(\mathbf{1}_N \otimes \mathbf{I}_K) & \mathbf{I}_N \otimes \widetilde{\boldsymbol{\varphi}}(1:K)^T \\ \mathbf{1}_N\widetilde{\boldsymbol{\varphi}}^T(1:K) & \widehat{\mathbf{T}} \\ \mathbf{O}_{N\times K} & \widehat{\mathbf{T}} \end{bmatrix}, \tag{121c}$$

$$\widehat{\mathbf{T}} = \text{diag}\left(\widetilde{\boldsymbol{\varphi}}(K+1:2K)^T, \widetilde{\boldsymbol{\varphi}}(2K+1:3K)^T, \ldots, \widetilde{\boldsymbol{\varphi}}(NK+1:K(N+1))^T\right).$$

REFERENCES

[1] P. Abouzar, D. G. Michelson, and M. Hamdi, "RSSI-based distributed self-localization for wireless sensor networks used in precision agriculture," *IEEE Trans. Wireless Commun.*, vol. 15, no. 10, pp. 6638–6650, Oct. 2016.

[2] T. L. T. Nguyen, F. Septier, H. Rajaona, G. W. Peters, I. Nevat, and Y. Delignon, "A Bayesian perspective on multiple source localization in wireless sensor networks," *IEEE Trans. Signal Process.*, vol. 64, no. 7, pp. 1684–1699, Apr. 2016.

[3] F. Yin, C. Fritsche, D. Jin, F. Gustafsson, and A. M. Zoubir, "Cooperative localization in WSNs using Gaussian mixture modeling: Distributed ECM algorithms," *IEEE Trans. Signal Process.*, vol. 63, no. 6, pp. 1448–1463, Mar. 2015.

[4] M. Z. Win, W. Dai, Y. Shen, G. Chrisikos, and H. V. Poor, "Network operation strategies for efficient localization and navigation," *Proc. IEEE*, vol. 106, no. 7, pp. 1224–1254, Jul. 2018.

[5] M. Z. Win, Y. Shen, and W. Dai, "A theoretical foundation of network localization and navigation," *Proc. IEEE*, vol. 106, no. 7, pp. 1136–1165, Jul. 2018.

[6] M. Z. Win, F. Meyer, Z. Liu, W. Dai, S. Bartoletti, and A. Conti, "Efficient multisensor localization for the internet of things: Exploring a new class of scalable localization algorithms," *IEEE Signal Process. Mag.*, vol. 35, no. 5, pp. 153–167, Sep. 2018.

[7] M. Naraghi-Pour and T. Ikuma, "EM-based localization of noncooperative multicarrier communication sources with noncoherent subarrays," *IEEE Trans. Wireless Commun.*, vol. 17, no. 9, pp. 6149–6159, Sep. 2018.

[8] J. Vander Hook, P. Tokekar, and V. Isler, "Algorithms for cooperative active localization of static targets with mobile bearing sensors under communication constraints," *IEEE Trans. Robot.*, vol. 31, no. 4, pp. 864–876, Aug. 2015.

[9] D. J. Peters, "A Bayesian method for localization by multistatic active sonar," *IEEE J. Ocean. Eng.*, vol. 42, no. 1, pp. 135–142, Jan. 2017.

[10] A. Farina and E. Hanle, "Position accuracy in netted monostatic and bistatic radar," *IEEE Trans. Aerosp. Electron. Syst.*, vol. AES-19, no. 4, pp. 513–520, Jul. 1983.

[11] S. Bartoletti, A. Giorgetti, M. Z. Win, and A. Conti, "Blind selection of representative observations for sensor radar networks," *IEEE Trans. Veh. Technol.*, vol. 64, no. 4, pp. 1388–1400, Apr. 2015.

[12] T. Le and N. Ono, "Closed-form and near closed-form solutions for TOA-based joint source and sensor localization," *IEEE Trans. Signal Process.*, vol. 64, no. 18, pp. 4751–4766, Sep. 2016.

[13] H. Shen, Z. Ding, S. Dasgupta, and C. Zhao, "Multiple source localization in wireless sensor networks based on time of arrival measurement," *IEEE Trans. Signal Process.*, vol. 62, no. 8, pp. 1938–1949, Apr. 2014.

[14] Y. T. Chan and K. C. Ho, "A simple and efficient estimator for hyperbolic location," *IEEE Trans. Signal Process.*, vol. 42, no. 8, pp. 1905–1915, Aug. 1994.

[15] K. C. Ho, "Bias reduction for an explicit solution of source localization using TDOA," *IEEE Trans. Signal Process.*, vol. 60, no. 5, pp. 2101–2114, May 2012.

[16] S. Tomic, M. Beko, and R. Dinis, "RSS-based localization in wireless sensor networks using convex relaxation: Noncooperative and cooperative schemes," *IEEE Trans. Veh. Technol.*, vol. 64, no. 5, pp. 2037–2050, May 2015.

[17] H. Shao, X. Zhang, and Z. Wang, "Efficient closed-form algorithms for AOA based self-localization of sensor nodes using auxiliary variables," *IEEE Trans. Signal Process.*, vol. 62, no. 10, pp. 2580–2594, May 2014.

[18] S. Tomic, M. Beko, and R. Dinis, "3-D target localization in wireless sensor networks using RSS and AOA measurements," *IEEE Trans. Veh. Technol.*, vol. 66, no. 4, pp. 3197–3210, Apr. 2017.

[19] Y. Li, G. Qi, and A. Sheng, "Performance metric on the best achievable accuracy for hybrid TOA/AOA target localization," *IEEE Commun. Lett.*, vol. 22, no. 7, pp. 1474–1477, Jul. 2018.

[20] J. Luo, X. Zhang, and Z. Wang, "A new passive source localization method using AOA-GROA-TDOA in wireless sensor array networks and its Cramér-Rao bound analysis," in *Proc. IEEE Int. Conf. Acoust., Speech, Signal Process.*, Vancouver, BC, Canada, May 2013, pp. 4031–4035.

[21] E. Hanle, "Survey of bistatic and multistatic radar," *Proc. Inst. Electr. Eng. F–Commun., Radar, Signal Process.*, vol. 133, no. 7, pp. 587–595, Dec. 1986.

[22] H. Yang and J. Chun, "An improved algebraic solution for moving target localization in noncoherent MIMO radar systems," *IEEE Trans. Signal Process.*, vol. 64, no. 1, pp. 258–270, Jan. 2016.

[23] L. Yang, L. Yang, and K. C. Ho, "Moving target localization in multistatic sonar by differential delays and Doppler shifts," *IEEE Signal Process. Lett.*, vol. 23, no. 9, pp. 1160–1164, Sep. 2016.

[24] S. Simakov, "Localization in airborne multistatic sonars," *IEEE J. Ocean. Eng.*, vol. 33, no. 3, pp. 278–288, Jul. 2008.
[25] M. Sandys-Wunsch and M. G. Hazen, "Multistatic localization error due to receiver positioning errors," *IEEE J. Ocean. Eng.*, vol. 27, no. 2, pp. 328–334, Apr. 2002.
[26] B. Sobhani, E. Paolini, A. Giorgetti, M. Mazzotti, and M. Chiani, "Target tracking for UWB multistatic radar sensor networks," *IEEE J. Sel. Topics Signal Process.*, vol. 8, no. 1, pp. 125–136, Feb. 2014.
[27] I. Ivashko, O. Krasnov, and A. Yarovoy, "Performance analysis of multisite radar systems," in *Proc. Eur. Radar Conf.*, Nuremberg, Germany, Oct. 2013, pp. 459–462.
[28] L. Rui and K. C. Ho, "Elliptic localization: Performance study and optimum receiver placement," *IEEE Trans. Signal Process.*, vol. 62, no. 18, pp. 4673–4688, Sep. 2014.
[29] N. H. Nguyen and K. Doğançay, "Optimal geometry analysis for multistatic TOA localization," *IEEE Trans. Signal Process.*, vol. 64, no. 16, pp. 4180–4193, Aug. 2016.
[30] M. Malanowski and K. Kulpa, "Two methods for target localization in multistatic passive radar," *IEEE Trans. Aerosp. Electron. Syst.*, vol. 48, no. 1, pp. 572–580, Jan. 2012.
[31] H. Godrich, A. M. Haimovich, and R. S. Blum, "Target localization accuracy gain in MIMO radar-based systems," *IEEE Trans. Inf. Theory*, vol. 56, no. 6, pp. 2783–2803, Jun. 2010.
[32] J. Shen, A. F. Molisch, and J. Salmi, "Accurate passive location estimation using TOA measurements," *IEEE Trans. Wireless Commun.*, vol. 11, no. 6, pp. 2182–2192, Jun. 2012.
[33] Y. Zhou, C. L. Law, Y. L. Guan, and F. Chin, "Indoor elliptical localization based on asynchronous UWB range measurement," *IEEE Trans. Instrum. Meas.*, vol. 60, no. 1, pp. 248–257, Jan. 2011.
[34] H. Yang, J. Chun, and D. Chae, "Two-stage localization method in multistatic radar systems," in *Proc. IEEE Radar Conf.*, Cincinnati, OH, USA, May 2014, pp. 1052–1056.
[35] M. Einemo and H. C. So, "Weighted least squares algorithm for target localization in distributed MIMO radar," *Signal Process., Elsevier*, vol. 115, pp. 144–150, Oct. 2015.
[36] L. Rui and K. C. Ho, "Efficient closed-form estimators for multistatic sonar localization," *IEEE Trans. Aerosp. Electron. Syst.*, vol. 51, no. 1, pp. 600–614, Jan. 2015.
[37] P. Stinco, M. S. Greco, F. Gini, and M. Rangaswamy, "Ambiguity function and Cramer-Rao bounds for universal mobile telecommunications system-based passive coherent location systems," *Proc. IET Radar, Sonar Navig.*, vol. 6, no. 7, pp. 668–678, Aug. 2012.
[38] G. Park, D. Kim, H. J. Kim, and H. Kim, "Maximum-likelihood angle estimator for multi-channel FM-radio-based passive coherent location," *Proc. IET Radar, Sonar Navig.*, vol. 12, no. 6, pp. 617–625, 2018.
[39] K. W. K. Lui, W. Ma, H. C. So, and F. K. W. Chan, "Semi-definite programming algorithms for sensor network node localization with uncertainties in anchor positions and/or propagation speed," *IEEE Trans. Signal Process.*, vol. 57, no. 2, pp. 752–763, Feb. 2009.
[40] J. A. Bhatti, T. E. Humphreys, and B. M. Ledvina, "Development and demonstration of a TDOA-based GNSS interference signal localization system," in *Proc. IEEE/ION Position, Location, Navig. Symp.*, Myrtle Beach, SC, USA, Apr. 2012, pp. 455–469.
[41] V. Antonyuk, I. Prudyus, V. Nichoga, and A. Kawalec, "Integration of passive coherent radar system into the passive TDOA system," in *Proc. 13th Int. Radar Symp.*, Warsaw, Poland, May 2012, pp. 354–358.
[42] S. M. Kay, *Fundamentals of Statistical Signal Processing: Estimation Theory*. Englewood Cliffs, NJ, USA: Prentice-Hall, 1993.
[43] F. Hiai and D. Petz, *Introduction to Matrix Analysis and Applications*. Berlin, Germany: Springer Science+Business Media, 2014.
[44] P. Stoica and K. C. Sharman, "Maximum likelihood methods for direction-of-arrival estimation," *IEEE Trans. Acoust., Speech, Signal Process.*, vol. 38, no. 7, pp. 1132–1143, Jul. 1990.
[45] K. C. Ho, X. Lu, and L. Kovavisaruch, "Source localization using TDOA and FDOA measurements in the presence of receiver location errors: Analysis and solution," *IEEE Trans. Signal Process.*, vol. 55, no. 2, pp. 684–696, Feb. 2007.
[46] F. Richter and G. Fettweis, "Base station placement based on force fields," in *Proc. IEEE Veh. Technol. Conf.*, Yokohama, Japan, 2012, pp. 1–5.
[47] W. Dai, Y. Shen, and M. Z. Win, "Energy-efficient network navigation algorithms," *IEEE J. Sel. Areas Commun.*, vol. 33, no. 7, pp. 1418–1430, Jul. 2015.
[48] Y. Shen, W. Dai, and M. Z. Win, "Power optimization for network localization," *IEEE/ACM Trans. Netw.*, vol. 22, no. 4, pp. 1337–1350, Aug. 2014.
[49] W. Dai, Y. Shen, and M. Z. Win, "Distributed power allocation for cooperative wireless network localization," *IEEE J. Sel. Areas Commun.*, vol. 33, no. 1, pp. 28–40, Jan. 2015.
[50] W. Dai, Y. Shen, and M. Z. Win, "A computational geometry framework for efficient network localization," *IEEE Trans. Inf. Theory*, vol. 64, no. 2, pp. 1317–1339, Feb. 2018.
[51] Z. Liu, W. Dai, and M. Z. Win, "Node placement for localization networks," in *Proc. IEEE Int. Conf. Commun.*, Paris, France, 2017, pp. 1–6.
[52] A. Sinha, T. Kirubarajan, and Y. Bar-Shalomb, "Optimal cooperative placement of GMTI UAVs for ground target tracking," in *Proc. IEEE Aerosp. Conf.*, Big Sky, MT, USA, Mar. 2004, pp. 1859–1868.
[53] B. Yang and J. Scheuing, "Cramer-Rao bound and optimum sensor array for source localization from time differences of arrival," in *Proc. IEEE Int. Conf. Acoust., Speech, Signal Process.*, Philadelphia, PA, USA, Mar. 2005, pp. 961–964.
[54] P. S. Bullen, *Handbook of Means and Their Inequalities*. New York, NY, USA: Springer, 2003.
[55] S. Kim, B. Ku, W. Hong, and H. Ko, "Performance comparison of target localization for active sonar systems," *IEEE Trans. Aerosp. Electron. Syst.*, vol. 44, no. 4, pp. 1371–1380, Oct. 2008.

Yang Zhang (S'19) was born in Liaoning, China. He received the B.S. degree in electronics and information engineering and the M.S. degree in signal and information processing from the Dalian University of Technology, Liaoning, China, in 2012 and 2015, respectively. He is currently working toward the Ph.D. degree with the Department of Electrical Engineering and Computer Science, University of Missouri-Columbia, Columbia, MO, USA. His research interests include multistatic radar/sonar localization, statistical and digital signal processing, and time delay estimation.

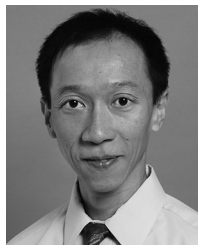

K. C. Ho (S'89–M'91–SM'00–F'09) was born in Hong Kong. He received the B.Sc. degree with first class honors in electronics, and the Ph.D. degree in electronic engineering in 1991 from the Chinese University of Hong Kong, Hong Kong, in 1988 and 1991, respectively. From 1991 to 1994, he was a Research Associate with the Royal Military College of Canada, ON, Canada. He joined the Bell-Northern Research, Montreal, Canada, in 1995 as a member of scientific staff. From September 1996 to August 1997, he was a faculty member with the Department of Electrical Engineering, University of Saskatchewan, Saskatoon, SK, Canada. Since September 1997, he has been with the University of Missouri, Columbia, MO, USA, and is currently a Professor with the Electrical Engineering and Computer Science Department. He is an inventor of 9 patents in USA and 13 patents in Canada, Europe, and Asia on geolocation and signal processing for wireless communications. His research interests include sensor array processing, source localization, subsurface object detection, wireless communications, and adaptive processing. He was active in the development of the ITU-T Standard Recommendations from 1995 to 2012. He was the Rapporteur of ITU-T Q15/SG16: Voice Gateway Signal Processing Functions and Circuit Multiplication Equipment/Systems from 2009 to 2012, and the Associate Rapporteur of ITU-T Q16/SG16: Speech Enhancement Functions in Signal Processing Network Equipment in 2012. He was the Editor for the ITU-T Recommendations G.160: Voice Enhancement Devices from 2006 to 2012, G.168: Digital Network Echo Cancellers from 2000 to 2012 and G.799.2: Mechanism for Dynamic Coordination of Signal Processing Network Equipment from 2004 to 2009. He was a Technical Chair of the IEEE International Conference on Acoustics, Speech, and Signal Processing 2016. He has served as the Past Chair (2015), the Chair (during 2013–2014), and the Vice-Chair (during 2011–2012) of the Sensor Array and Multichannel Technical Committee of the IEEE Signal Processing Society. He was on the organizing committees of the IEEE SAM 2008 Workshop and the IEEE CAMSAP 2011. He was an Associate Editor for the IEEE TRANSACTIONS ON SIGNAL PROCESSING (during 2009–2013 and 2003–2006) and the IEEE SIGNAL PROCESSING LETTERS (during 2004–2008). He was a recipient of the Senior Faculty Research Award in 2014 and 2009, the Junior Faculty Research Award in 2003, and the Teaching Award in 2006 from the College of Engineering, University of Missouri.